CHALMERS

Evaluation of the effect of impact under installation on the performance of concrete cover for protection of ductile iron pipe

– Analysis of the possible corrosion caused by the Göteborg ground

Master of Science Thesis in the Master's Programme Structural Engineering and Building Performance Design

HÉCTOR PÉREZ GARCÍA

Department of Civil and Environmental Engineering
Division of Building Technology
Building Materials
CHALMERS UNIVERSITY OF TECHNOLOGY
Göteborg, Sweden 2012

Master's Thesis 2012:146

MASTER'S THESIS 2012:146

Evaluation of the effect of impact under installation on the performance of concrete cover for protection of ductile iron pipe

– Analysis of the possible corrosion caused by the Göteborg ground

Master of Science Thesis in the Master's Programme Structural Engineering and Building Performance Design

HÉCTOR PÉREZ GARCÍA

Department of Civil and Environmental Engineering
Division of Building Technology
Building Materials
CHALMERS UNIVERSITY OF TECHNOLOGY
Göteborg, Sweden 2012

Evaluation of the effect of impact under installation on the performance of concrete cover for protection of ductile iron pipe

– Analysis of the possible corrosion caused by the Göteborg ground

Master of Science Thesis in the Master's Programme Structural Engineering and Building Performance Design

HÉCTOR PÉREZ GARCÍA

Examensarbete / Institutionen för bygg- och miljöteknik,
Chalmers tekniska högskola 2012:146

Department of Civil and Environmental Engineering
Building Technology
Building Materials
Chalmers University of Technology
SE-412 96 Göteborg
Sweden
Telephone: + 46 (0)31-772 1000

Cover:
Example of impact test ZM-U Fabrikstest – 3.B specimen.

Chalmer reproservice / Department of Civil and Environmental Engineering
Göteborg, Sweden 2012

Evaluation of the effect of impact under installation on the performance of concrete cover for protection of ductile iron pipe

– Analysis of the possible corrosion caused by the Göteborg ground

Master of Science Thesis in the Master's Programme Structural Engineering and Building Performance Design

HÉCTOR PÉREZ GARCÍA
Department of Civil and Environmental Engineering
Division of Building Technology
Building Physics
Chalmers University of Technology

ABSTRACT

This dissertation presents a study of factors influencing the service life of ductile iron pipes exposed to soil. The aim of this examination work is to evaluate the effect of impact under installation phase on the performance of concrete cover for protection of the ductile iron pipe for water supplying.

In this project a special focus was put on the performance of concrete cover (VRS-ZM pipe) and epoxy coating (VRS-PRO pipe) with regard to the protection of iron pipe from corrosion risk.

The experimental part of the study involved the comparison between different specimens after impact levels simulating the installation in order to evaluate the performance of the cover and coating, which protects the ductile iron pipe. Special attention was taken in the analysis of the behaviour and the possible damage of the zinc layer, which protects the iron ductile against corrosion. Thus, two types of K9 pipe were studied, VRS-ZM and VRS-PRO.

The effect of the possible corrosion of the ductile iron and the zinc degradation was studied through different methods. First, the pipes were applied in a salt solution bath (5% NaCl) to measure the potential evolution and the current with respect to the time. This method was changed after one month because it was too slow to get results in the short term. Therefore, it was chosen to analyse the zinc layer measuring the potential between different points of the surface and ductile iron. Later, the current passing through different parts of the pipe surface, with particular attention to the impact area, was measured by applying different potentials. This results in the estimation of resistance.

The results show the importance of an exterior cover layer for protecting the ductile iron under corrosion. Besides, the concrete cover may have good performance under high impacts ($\leq$180 J) for protecting the ductile iron against corrosion risk.

Key words: Concrete cover, corrosion, epoxy coating, ductile iron pipe, zinc

Table of contents

Preface

In this study, the performance of concrete cover and epoxy coating for protection of ductile iron pipe against impact damage was evaluated, especial focus on corrosion factors. The tests have been carried out from February 2012 to September 2012 at the Department of Civil and Environmental engineering, Chalmers University of Technology. The project has been supported by Götegorg Vatten company.

This project has been carried out under the supervision of Tang Luping, (professor and research group leader of Building Materials), Fredrik Johansson (Göteborg Vatten - Projekt och Teknik – Dricksvattendistribution) and Luis Pallares (University professor at Universistat Politècnica de Valencia – PDI). I would like to express my thanks to my supervisors for taking care of me and for valuable information that have helped me. I would also like to thank to my family and friends for their support during my work

I declare that I worked out the thesis on my own, using the literature stated in references.

Göteborg, September 2012

Héctor Pérez García

Nomenclature

B. Back [-]

Rp^{-1}. Inverse of the polarization resistance [Ohm^{-1}]

E_{imp}. Impact energy [J]

E_{corr}. Corrosion potential [mV]

I. Current in the circuit [mA]

I_{corr}. Corrosion current [$\mu A/cm^2$]

FBE. Fusion Bonded Epoxy

L. Left [-]

L1. External Left size [-]

M. Middle [-]

R. Right size [-]

R1. External Right size [-]

R_A. Amperemeter resistivity [Ohm]

R_s. Resistance of the specimen [Ohm]

R_c. Resistivity of the concrete [kOhm·cm]

SCC. Stress-corrosion cracking

V. Potential [V]

V'. Voltage across the electrode and the iron [V]

V_0. Power supply [V]

VRS-PRO. Pipe ductile iron- Class K9 according to EN-545. Int. concrete coating, ext. zinc and epoxy. Pipe length (L) 6 meters.

VRS-ZM. Pipe ductile iron - Class K9 according to EN-545. Int. concrete coating, ext. zinc and concrete. Pipe length (L) 6 meters.

g. Acceleration of gravity [m/s^2]

m. Weight of element [kg]

v_{corr}. Rate of corrosion [µm/year]

y. Height of element [m]

δ. Delta phase [-]

η. Eta phase [-]

γ. Gamma phase [-]

ξ. Zeta phase [-]

1 INTRODUCTION

1.1 Background

After more than 30 years without any change in the pipelines in Göteborg, these have become obsolete. These old pipes are composed by different layers: the inner layer by concrete, the intermediate one by ductile iron and the surface by an asphalt layer. Nowadays the old pipelines are facing replacement gradually. Thereby, there was an interest to study a new type of pipe regarding the service life under a possible corrosion environment.

Nowadays a kind of pipe contains a zinc layer to protect the ductile iron, e.g. the K9 (SS - EN 545-2006) from Gustavsberg Rörsystem with different coating covers. The VRS-ZM pipe is formed with an interior layer of concrete, ductile iron, zinc and a concrete exterior layer; and the VRS-PRO pipe, with the same conditions without concrete cover, but with an epoxy coating layer.

Thus, a possible impact during the installation of the new pipes affects the performance of the coating cover for protection the zinc layer and the ductile iron.

The most obvious consequence of the damage of the coating cover and the zinc layer is the deterioration by corrosion of the ductile iron pipe, leading to leakage of water. Knowledge, especially of the long-term effects of protection layer (concrete, zinc, epoxy...) used to increase the service life of iron ductile pipes, is inadequate. The lack of basic knowledge of substantial corrosion processes prior to and after maintenance and repair measures is a drawback in structural rehabilitation. This lack of knowledge causes unexpected expenses and even fatal errors when decisions are made about the methods and time of extending the service life of ductile iron pipes.

1.2 Research problem

The function of the concrete cover in the pipe is to protect the zinc layer under impacts and the loads will be applied to itself and protect the pipe against chemical attacks. Anyway, a lack of concrete in the layer increases the possible damage of zinc and consequently the corrosion of the ductile iron. Thus, a lack of protection layer increases the risk of corrosion and the possible deterioration of the ductile iron by corrosion affecting the service life of the pipeline.

In that case the research problem focuses on a study to estimate the damage of the protection layers of the ductile iron after an impact. Thus, this raises the need to assess the possible corrosion risk of the ductile iron in absence of protection layer, or damaged protection layer.

1.3 Aim and objectives of the research

The aim of this study was to evaluate the effect of impact under installation phase on the performance of concrete cover for protection of the ductile iron pipe for water supplying. Moreover, one of the objectives was to analyse the factors influencing the service life of iron ductile pipes, especially on corrosion conditions. Finally, another objective in the study was to develop a method for estimating the service life of the pipe with regard to ductile iron corrosion.

1.4 Research methods

The study includes both literature review and experimental work. The literature review was focused on two points: First, on the external corrosion protection of the buried pipes for water supplying, with special attention to the zinc properties, the thickness and formation of the zinc coating, the formation of the passive layer of the hot-dip galvanised steel and the influence of the coating (concrete and epoxy) cover; secondly, it was focused on the evaluation of type of soil against corrosion on the buried pipes. The main topics include corrosion mechanisms, mechanical properties, concrete properties, epoxy properties, steel properties, properties of the galvanising method, the formation of the zinc coating and the evaluation of corrosive soils.

For developing the evaluation a kind of pipe with coating cover above a zinc layer to protect the ductile iron was used, the K9 (EN 545-2006) from Gustavsberg Rörsystem.[1] The first one was the VRS-ZM pipe formed with an interior layer of concrete (3.5 mm – ISO 4179:2005), ductile iron (6 mm – SS - EN 545:2006), zinc (200 gr/m^2 – ISO 8179-2) and a concrete exterior layer (5 mm – DIN 30 674). The other pipe used to compare the results was the VRS-PRO, without the exterior concrete cover, but with an epoxy layer (120 μm – ISO 8179-1:2004). Both pipes were 150 mm of diameter.

The experimental work was focused on simulation of the installation impact and evaluation of the performance of the specimens after impact. The impact test was based on ZM-U Fabrikstest (7.2.3 SS-EN 15542:2008). This test exposes a free fall from one meter of a weight; this weight depends on the concrete thickness. At the beginning, it was decided to use the reference weight (VRS-ZM) in order to test all the specimens from one, two and three meters. A radial cut test was also applied for VRS-ZM and a sanding test for VRS-PRO. Thus, the results were analyzed with a visual inspection between the test specimens and the generic specimens.

The study of the zinc behavior and the possible corrosion of the iron ductile of the pipes was done after the impact test. First, the study was focused on salt bath (5% solution of NaCl), and the open circuit potential and the current with respect to the time were measured. After one month, no significant change from the initial values, but just a small variation was observed. Thus the approach to the service life of the Zn-

[1] Gustavsberg Rörsystem (2005). *VRS SYSTEM - Ett komplett system rör och rördelar med dragsäkra fogar.*

Fe was changed to the measurement of the potential (V) difference between different points of the surface and ductile iron. Afterwards, the current passing through different parts of the pipe surface, with particular attention to the impact area, was measured by applying different potentials. This results in the estimation of resistance.

1.5 Limitations of the research

The main parameters studied were the damage degree of the coating cover (concrete-VRS-ZM and epoxy-VRS-PRO) and the possible consequences on the zinc coating, which protects the ductile iron. The research was focused on the evolution of the potential difference of the zinc layer of the different specimens. The generic specimens were compared to the others specimens with different level of damage.

Due to the lack of model and standard test methods for service life of ductile iron pipe, this study was limited to the laboratory test as a pilot trial for estimation of corrosion risk of the pipe subjected to impacts.

Furthermore, the analysis of the possible corrosion caused by the Göteborg soil has been developed according to studies by Korrosioninstutet (KIMAB). Thus, the soil conditions could change depending on the place where the pipe is installed. Consequently, specific information about the corrosivity of a soil is needed to test the corrosion under the parameters of the soil and evaluate the possible consequences that would happen on the ductile iron pipes during their service life.

2 EXTERNAL CORROSION PROTECTION FOR DUCTILE-IRON PIPES

For several years, buried pipelines were installed without thinking of the need for external corrosion protection. Methods of corrosion prevention were non-existent because the causes were not well understood. The solutions adopted were to repair and replace the pipelines where the soil affected the external corrosion. This measure was accepted for utilities, although it was an expensive solution to corrosion problems.

Nowadays, buried pipelines can be installed practically in any kind of soil without major problems in that external corrosion. New technologies can protect the pipe under corrosive conditions and effective mitigation of corrosion when it is economically warranted. Anyway corrosion is a complex topic; good corrosion knowledge would permit to design an optimal solution in order to reduce failures and unnecessary costs.

2.1 Basic corrosion

The degeneration of an element or its attributes due to a reaction with its ambience is known as corrosion.[1] For several metals its elemental form is unoxidized, but due to the chemical reduction of the oxides, habitually the corrode form is the typical.[2] The corrosion is a process on which a metal, that is exposed, changes to its more stable form.

Moreover, for corrosion to take place a chemical reaction and a flow of electrical current are needed, namely an electrochemical process.[3] Usually the corrosion cell contains these elementary constituents: anode, cathode, electrolyte, and a return current path. In the corrosion process a metallic path connects electrically an anode and a cathode, which have to be dipped in an ionized electrolyte that is electrically conductive.[4] Besides, between the cathode and the anode there must be an electrical potential.

Thus, the soil can act as electrolyte in buried pipelines giving rise to potential differences. Hence, the electrons flow from the lower potential location (anode) through the metallic structure to higher potential location (cathode). The reactions happens to drive the current from the element to the electrolyte are chemical process. The current leaves the metal and enters the electrolyte at the anode where oxidation

[1] NACE (1984). *Corrosion Basics: An Introduction*. Houston, Texas: National Association of Corrosion Engineers.
[2] NACE (1984). *Corrosion Basics: An Introduction*. Houston, Texas: National Association of Corrosion Engineers.
[3] American Water Works Association (AWWA), (2009). *Ductile-Iron Pipe and Fittings - Manual of Water Supply Practices, M41. (3rd Edition)*, p. 166.
[4] Peabody, A.W. (1967). *Control of Pipeline Corrosion*. Houston, Texas: National Association of Corrosion Engineers.

reactions occur. When the electrons leave the electrolyte and enter the metal, reduction reactions occur at the cathode. The oxidation reactions take place; consequently corrosion happens at the anode. Usually, two basic types of corrosion can occur on buried pipes: galvanic corrosion and electrolytic corrosion.[1]

2.1.1 Galvanic corrosion

A corrosion current produced by two dissimilar metals dipped in a single uniform electrolyte can form a galvanic corrosion cell. In a similar way, the galvanic corrosion cell can be formed in a solid electrolyte of uneven configuration by similar metals. In both, the four basic constituents must take place in order to perform corrosion.[2]

- Dissimilar Metals. The *Figure 2.1* exemplifies how the corrosion current is generated by two different metals (iron and copper) electrically connected and dipped in a common, uniform electrolyte, forming a galvanic cell. The potential difference between the two metals will cause the current flow from the anode (iron) through the electrolyte to the cathode (copper) and back from the anode (iron) through the electrical connection, when the cell is connected in a circuit. In a contrary way, with a direction opposite to the conventional current flow, electrons migrate from the anode (iron) through the electrical connection to the cathode (cooper). The anode loses electrons, consequently positively charged iron atoms of the anode combine with the negatively charged hydroxyl ions (OH^-) in the electrolyte to form $Fe(OH)_2$, which have to react to form $Fe(OH)_3$. Corrosion appears due to the degradation of the metal anode surface by loss of iron atoms.[3]

Thus, a cumulus of negative charged electrons (from the anode) are at the cathode, these electrons attract positively charged hydrogen ions (H^+) to form hydrogen gas (H_2); Nevertheless, the cathode is preserved, it has no any loss of material. Usually, the electrons flow from the anode to the cathode through the electrical connection; the current leaves the anode, where that metal is degraded, to enter the electrolyte; and the cathode, that gets the current by the electrolyte, is not damaged.[4]

The rate of corrosion in any galvanic cell can be affected by the reactions that occur at the cathode and the anode. The corrosion can be affected, in soils, by cumulus of corrosion by-products; especially in dry soils the corrosion process can be stopped or interrupted preventing the transport of electrons into the electrolyte.[5]

---

[1] American Water Works Association (AWWA), (2009). *Ductile-Iron Pipe and Fittings - Manual of Water Supply Practices, M41. (3rd Edition)*, p. 166.
[2] American Water Works Association (AWWA), (2009). *Ductile-Iron Pipe and Fittings - Manual of Water Supply Practices, M41. (3rd Edition)*, p. 166.
[3] American Water Works Association (AWWA), (2009). *Ductile-Iron Pipe and Fittings - Manual of Water Supply Practices, M41. (3rd Edition)*, p. 166-167.
[4] American Water Works Association (AWWA), (2009). *Ductile-Iron Pipe and Fittings - Manual of Water Supply Practices, M41. (3rd Edition)*, p. 167.
[5] American Water Works Association (AWWA), (2009). *Ductile-Iron Pipe and Fittings - Manual of Water Supply Practices, M41. (3rd Edition)*, p. 167.

Thus, the severity of corrosion is influenced by the chemical composition of the electrolyte and the materials acting as the cathodic and anodic electrodes in a corrosion cell.[1] *(Fig 2.1)*

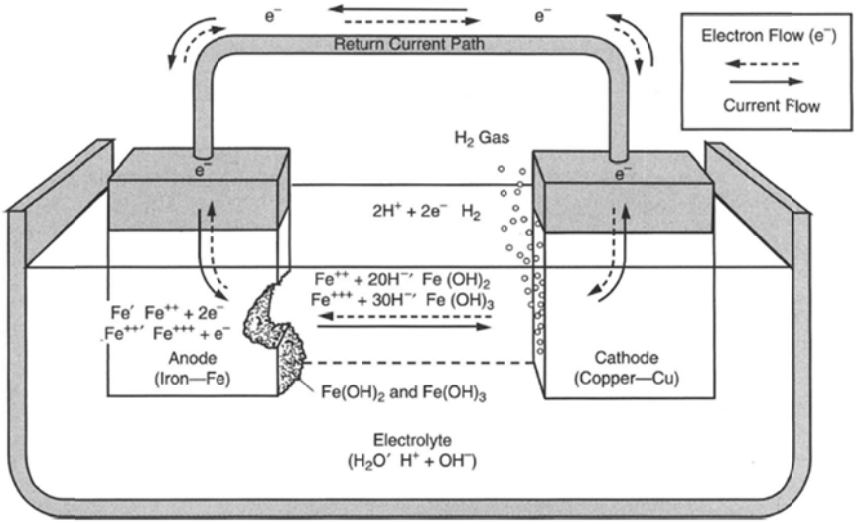

Figure 2.1. Chemical reactions in a typical galvanic corrosion cell.[2]

- Galvanic series. The current flow is generated by the difference in potential between copper and iron as *Figure 2.1* shows. The copper is protected and the iron is attacked. Anyway, while the iron is protected, another metal connected in circuit with iron might be attacked as well. Thus, it is important to know which metal will act as the anode and which metal will act as the cathode, in a galvanic cell created by similar metals.[3]

- Non-uniform Electrolytes. When similar metals are exposed to a solid electrolyte of uneven composition, galvanic corrosion can also occur. Usually, this kind of corrosion is less aggressive than the other types of corrosion.

2.1.2 Electrolytic corrosion

Furthermore, another type of corrosion is the electrolytic corrosion. This is the opposite of the galvanic corrosion; electrolytic corrosion also contains a flow of current through an electrolyte and electrochemical reactions happen. In galvanic corrosion there is no outside current involved. In electrolytic corrosion, for the current flowing,

[1] American Water Works Association (AWWA), (2009). *Ductile-Iron Pipe and Fittings - Manual of Water Supply Practices, M41. (3rd Edition)*, p. 167.
[2] American Water Works Association (AWWA), (2009). *Ductile-Iron Pipe and Fittings - Manual of Water Supply Practices, M41. (3rd Edition)*, p. 167.
[3] American Water Works Association (AWWA), (2009). *Ductile-Iron Pipe and Fittings - Manual of Water Supply Practices, M41. (3rd Edition)*, p. 168.

an external electric energy is needed. The final result is the same as the result of the galvanic corrosion: the anode is degraded by a flow of electric current.[1]

2.1.3 Microbiologically influenced corrosion

The effect on corrosion by soil bacteria is known by microbiologically influenced corrosion (MIC). Certain bacteria can reduce any sulfates consuming hydrogen in the process, these bacteria can exist with absence of oxygen in buried conditions. The corrosion process can be faster due to the depolarization of the cathodic areas by consumption of hydrogen giving rise a galvanic corrosion cell, which will increase the degradation of the metal. When corrosion cell exists, the bacteria are more damaging.[2]

2.1.4 Rate of corrosion

For buried pipes it is necessary to control the presence of corrosion cells and its rate of corrosion, because it can be an important problem. The degree of the current is directly connected with several factors as size, magnitude of potential difference and the physical and thermodynamic characteristics at the metal-electrolyte interface at the cathode and anode areas; and the electrical resistance of the various current paths, which have an influence on the chemical reaction rate. At the anode and cathode, chemical reactions are formed, the metal transfers current to the electrolyte and vice versa. The evolution of this process changes the properties of the environment so as to limit further corrosion reactions. This process is known as passivation and depends on the soil and the metal properties. Consequently, corrosion could not appear with presence of corrosion cells.[3]

The most common type of corrosion can be found in buried pipes, it is galvanic corrosion. In these conditions, the galvanic cells form a low potential difference giving rise to formation of corrosion reactions, usually in dissimilar electrolytes, which have an influence on the rate of corrosion.[4]

2.2 Zinc deterioration

The most used material for protecting the steel or iron is the zinc. During aqueous corrosion the coating layer of zinc often form a porous β-FeOOH layer and duplex of Fe_3O_2 and Fe_2O_3.[5] Usually, the elements with galvanized steels (like buried pipes) in

[1] Motor Boating & Sailing (1992), *ISSN 0027-1799, 05/1992*, Volume 169, Issue 5, p. 107.
[2] American Water Works Association (AWWA), (2009). *Ductile-Iron Pipe and Fittings - Manual of Water Supply Practices, M41. (3rd Edition)*, p. 171.
[3] American Water Works Association (AWWA), (2009). *Ductile-Iron Pipe and Fittings - Manual of Water Supply Practices, M41. (3rd Edition)*, p. 171.
[4] American Water Works Association (AWWA), (2009). *Ductile-Iron Pipe and Fittings - Manual of Water Supply Practices, M41. (3rd Edition)*, p. 171.
[5] Carlos Castillo (2011). *The Electrochemical Behaviour of Zinc*, p. 1.

external environments can be found in wet and dry conditions. Several tests have demonstrated that the corrosion reactions are accelerated, in an initial moment, at wet/dry cycles, then the corrosion rate is decreases till being constant for galvanized steel.[1]

The zinc coating acts in two ways to protect the steel; first as a layer that isolates the steel from the corrosive substance and the other one as a sacrificial anode. The passive layer is formed of the zinc coating into aqueous solution; generally it is formed by ZnO. The reactions that happen on the Zn and Fe have an influence on the protection of the underlying layer of the steel by the anodic form of zinc.

2.2.1 Corrosion of zinc

The behaviour of the zinc layer to protect steels with wet/dry cycles follows the next sequence: initially it corrodes at an accelerated rate, afterwards the rate decreases progressively and finally remains stable. In the first contact with the substance, ZnO layer appears to cover the surface of galvanised steel, the decomposition of the passive layer rises to the accelerated corrosion rate; moreover the zinc dissolves due to chloride ions concentrated during the drying period.[2] Furthermore, the corrosion of the underlying steel starts when the red rust (mainly β-FeOOH) appears during the progressive decrease of the corrosion rate.[3] Yadav et al. demonstrated that for extend periods of drying cycles of the specimens the inverse of the polarization resistance (R_p^{-1}), which is proportional to the corrosion rate, decreases quickly.[4] In the test it was shown that the appearance of red rust was found after the maximum of R_p^{-1}. Yadav´s test also showed the influence of the drying period with the thickness loss of the galvanised coating: the specimens with more drying time developed higher thickness loss of coating than the specimens with less drying time. For large drying time the specimen exposes the zinc surface to more chlorides, consequently pitting corrosion arrives to the zinc-steel layer[5].

The next corrosion products for zinc (with a layer of about 500 μm thickness - in wet and dry cycles in a 0.05 M NaCl solution) were identified by Yadav et al.: $Zn(OH)_2$, $ZnCl_2{\cdot}6Zn(OH)_2$, $ZnCl_2{\cdot}4Zn(OH)_2$ following a sequence as the concentration of chloride and hydrogen ions increase. In the drying periods the corrosion products appeared, when the evaporation of the water heads to the concentration of chloride ions. With a

[1] Yavad, A. P., A. Nishikata, and T. Tsuru (2004). *Electrochemical impedance study on galvanized steel corrosion under cyclic wet-dry conditions – influence of time of wetness.* Corrosion Science, p. 169-181.
[2] Yavad, A. P., A. Nishikata, and T. Tsuru (2004). *Electrochemical impedance study on galvanized steel corrosion under cyclic wet-dry conditions – influence of time of wetness*. Corrosion Science, p. 169-181.
[3] Yavad, A. P., A. Nishikata, and T. Tsuru (2004). *Electrochemical impedance study on galvanized steel corrosion under cyclic wet-dry conditions – influence of time of wetness.* Corrosion Science, p. 169-181.
[4] Yavad, A. P., A. Nishikata, and T. Tsuru (2004). *Electrochemical impedance study on galvanized steel corrosion under cyclic wet-dry conditions – influence of time of wetness*. Corrosion Science, p. 169-181.
[5] Yavad, A. P., A. Nishikata, and T. Tsuru (2004). *Electrochemical impedance study on galvanized steel corrosion under cyclic wet-dry conditions – influence of time of wetness*. Corrosion Science, p. 169-181.

variation of chloride ion content, different Zn precipitate as $ZnCl_2{\cdot}4Zn(OH)_2$, ZnO, $Zn(OH)_2$ and $ZnCO_3$ could be formed.[1]

In the beginning of corrosion a solution as Zn^{2+} is formed where the zinc coating is dissolved acting as a sacrificial anode. The Zn^{2+} dispersed through the pores corrosion products, which are developed on the zinc surface. While zinc surface acts as an anode, thicker layer products (mostly $ZnCl_2{\cdot}4Zn(OH)_2$) appear, however transfer of the mass of O_2 and Zn^{2+} is not stopped by the corrosion products.[2] In the process of the dissolution of the zinc the anodic areas have a higher rate active than the cathodic areas, despite the fact that on the whole surface the reduction of oxygen is developed at the same rate. The dissolution of the zinc and the corrosion changes (from anode to cathode) are stopped when the corrosion starts to appear on the Zn-Fe layer, due to the fact that Zn-Fe layer has a higher positive potential than the zinc. Finally, while the zinc is covered with sufficient electrolyte, it can still act as sacrificial anode.[3] *(Fig 2.2)*

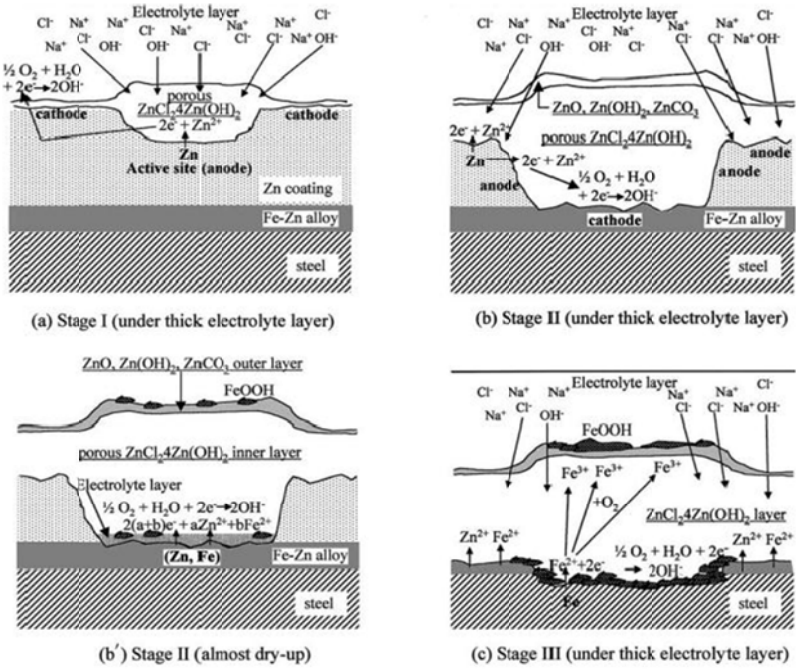

Figure 2.2. Illustration of corrosion mechanism of galvanized steel.[4]

El-Mahdy et al. developed some tests to check the corrosion mass loss in a wet/dry cycles (15 cycles – 1 hour immersed and 7 hours of drying) in a solution of 0.05 M NaCl for steel. Firstly in an area the rate of loss of mass was accelerated till the red rust was recognisable to the naked eyed, this means that the corrosion appears on the

[1] Yavad, A. P., A. Nishikata, and T. Tsuru (2004). *Electrochemical impedance study on galvanized steel corrosion under cyclic wet-dry conditions – influence of time of wetness*. Corrosion Science, p. 169-181.
[2] Carlos Castillo (2011). *The Electrochemical Behaviour of Zinc*, p. 6.
[3] Carlos Castillo (2011). *The Electrochemical Behaviour of Zinc*, p. 6.
[4] Yavad, A. P., A. Nishikata, and T. Tsuru (2004). *Electrochemical impedance study on galvanized steel corrosion under cyclic wet-dry conditions – influence of time of wetness*. Corrosion Science, p. 169-181.

underlying steel. Secondly, the rate of loss of mass decreased, after the red rust had appeared. [1]

Aal and Wanees developed several trials to test Zn in near neutral in Na_2SO_4 solutions [0.0005-0.1 M]. The formation point of ZnO was defined by the polarization curve. Once ZnO was formed, after a maximum the potential evolves negatively, it means that the passive layer breaking down the pitting corrosion is initiating on the zinc surface.[2]

Gouda et al. developed experiments in two groups, depending on the anion concentration (from 10^{-6} to 5 M) and time, to check the potential of pure zinc. The first group formed by SO_4^{2-}, Cl^-, Br^-, I^-, ClO_4^- and NO_3^- ; when the concentration of the anions increases, the potential of the zinc electrode decreases due to a difference between the cathodic and anodic reactions. The oxide film layer is reconstructed by oxygen reduction, once the same film was destroyed by the anion concentration. The rate of oxygen reduction increases to counter the accelerated corrosion.[3]

The other group was formed by CrO_4^{2-}, $H_2PO_4^-$, and NO_2^-. The potential developed, at low concentrations, by the zinc electrode depends on the type of anion, but not on the concentration. In certain concentration, depending on the salt, the potential starts to depend on the concentration and corrosion is inhibited when the potential changes to positive.[4]

2.2.2 Corrosion of underlying steel

Yadav et al. demonstrated in their study on the corrosion of zinc coating for steel on wet/dry cycles the appearance of red rust was found after the maximum of R_p^{-1} in 0.5 M NaCl solution. Their result showed zinc remains on the specimen when the corrosion takes place on the underlying steel. Thus, the steel is partially in contact to the chlorides solution after the maximum of R_p^{-1}. With short times of drying, the thickness loss will be higher than with large times, in which the corrosion will appear to the zinc-steel layer before. Thus, for the red rust to appear and for the corrosion of the underlying steel the inhibition of zinc is required.[5] On the drying time, a region around the steel can function as a sacrificial anode if the surface of the specimen is involved with a layer of electrolyte solution.[6]

---

[1] El-Mahdy, Gamal Ahmed, Atsushi Nishikata, and Tooru Tsuru (2000). *Electrochemical corrosion monitoring of galvanized steel under cyclic wer-dry conditions*. Corrosion Science, p.183-194.

[2] Aal, E.E. Abd El, and S. Abd El Wanees (2009). *Galvanostatic study of the breakdown of Zn passivity by sulphate anions*. Corrosion Science, p.1780-1788.

[3] Gouda, V. K., M. G. A. Khedr, and A. M. Shams El Din. (1967). *Role of anions in the corrosion and corrosion-inhibition of zinc in aqueous solutions*. Corrosion Science, p.221-230.

[4] Gouda, V. K., M. G. A. Khedr, and A. M. Shams El Din. (1967). *Role of anions in the corrosion and corrosion-inhibition of zinc in aqueous solutions*. Corrosion Science, p.221-230.

[5] Carlos Castillo (2011). *The Electrochemical Behaviour of Zinc*, p. 11.

[6] Yavad, A. P., A. Nishikata, and T. Tsuru (2004). *Electrochemical impedance study on galvanized steel corrosion under cyclic wet-dry conditions – influence of time of wetness*. Corrosion Science, p. 169-181.

Moreover, the red rust appeared when E_{corr} had lower potential values than ordinary steels. In these potentials zinc coating works as cathodic protection. Thus, when the zinc starts to evolve, the steel corrodes as localized.[1]

R. P. Vera Cruz et al. showed as just before to dry the specimen completely, pitting corrosion and its growth starts to appear, in this moment a thin layer of electrolyte covers the specimen. When the specimen (dried) is dipped again,
the process of re-passivation takes place.[2]

The association of amorphous ferric oxides and hydroxides, ferric oxyhydroxides and magnetite form the steel rust.[3] Ishikawa et al. showed that $Fe(OH)_2$ reacts with the oxyhydroxides α-FeOOH (goethite), β-FeOOH (akaganeite) and γ-FeOOH (lepidocrocite) to produce Fe_3O_4 (magnetite), also recognised as $FeO{\cdot}Fe_2O_3$ (the most ordinary corrosion product in anaerobic conditions). $Fe(OH)_2$ will react with the ferric oxyhydroxides to produce usually Fe_3O_4 in the order of β-FeOOH > γ-FeOOH > α-FeOOH. Metal ions such as Cu(II) can minimize the particle growth and crystallization of goethite and lepidocrocite, and Ti(IV) can interrupt the formation of akaganeite. During the process of corrosion, the most stable ferric oxyhydroxides is β-FeOOH.[4]

Usually, in chloride environments akaganeite (β-FeOOH) is found as a corrosion substance in steels.[5] Thus, if the content of β-FeOOH on the surface decreases, it can reduce the corrosion rate of weathering steels, which is formed with less copper than normally.[6]

2.3 Galvanised pipes with concrete cover. Durability of hot-dip galvanised

In aggressive conditions the propagation of corrosion is delayed by zinc as the experience deduced after many years shows. Furthermore, the cracking and spalling of the concrete cover and rust damage formed on the surface of the structure are decreased by galvanisation. The galvanised steel resistance against failures, such as a too thin concrete cover, insufficient compacting or poor curing of the concrete, is better than the ordinary steel one. The steel is protected by zinc before concreting.[7] In carbonated concrete the chloride attack is less damaging in galvanised steel than

[1] Yavad, A. P., A. Nishikata, and T. Tsuru (2004). *Electrochemical impedance study on galvanized steel corrosion under cyclic wet-dry conditions – influence of time of wetness*. Corrosion Science, p. 169-181.
[2] Vera Cruz, R. P., A. Nishikata, and T.Tsuru (1996). *AC Impedance monitoring of pitting corrosion of stainless steel under wet-dry cyclic condition in chloride-containing environment*. Corrosion Science, p.1397-1406.
[3] Carlos Castillo (2011). *The Electrochemical Behaviour of Zinc*, p. 12.
[4] Ishikawa, Tatsuo, Minori Kumagai, Akemi Yasukawa, Kazuhiko Kanduri, Takenori Nakayama, and Fumio Yuse (2002). *Influence of metal ions on the formation of γ-FeOOH and magnetite rust*. Corrosion Science, p.1073-1086.
[5] Carlos Castillo (2011). *The Electrochemical Behavior of Zinc*, p. 13.
[6] Ishikawa, Tatsuo, Sho Miyamoto, Kazuhiko Kanduri and Takenori Nakayama (2005). *Influence of anions on the formation of β-FeOOH rust*. Corrosion Science, p.2510-2520.
[7] Yeomans, S.R. (1994). *A Conceptual Model for the Corrosion of Galvanized Reinforcement in Concrete*.

ordinary steel; the zinc has a low rate of corrosion because that zinc-coated steel in concrete remains passivated to a pH level around 9.5. Nevertheless, the corrosion of a zinc coating may be affected by the severity of the corrosive environment, the quality of the concrete, and the internal structure of the zinc layer.[1] Moreover, the corrosion is not stopped by zinc, but zinc itself reduces it.

2.3.1 Influence of steel material

Hot-dip galvanising consists of introducing the steel, non-heat and clean, in a bath of molten zinc at around 440-470 ºC. As a result, a metallurgical reaction between the steel and the zinc takes place, which produces a coating on the steel. A coating on the steel is produced by the metallurgical reaction, the coating made up of a series of iron-zinc alloy phases (gamma (γ), delta (δ), and zeta (ξ)); on the outer surface the phase of eta (η) is created and the other phases are developed from the steel-zinc interface up to this surface *(Fig 2.3)*.[2] Different factors influence the thickness of the zinc coating, such as the dipping temperature, the dipping time and the chemical composition of the steel. Other elements like carbon, manganese, phosphorus, and especially silicon in the steel affect the structure of the zinc coating that is formed. The thickness of the zinc coating (particularly the eta (η) phase) increases and the iron content of the zinc phases also tends to increase when the content of silicon in the steel increases. Changing the dipping time, the thickness of the zinc coating can be controlled. [3,4]

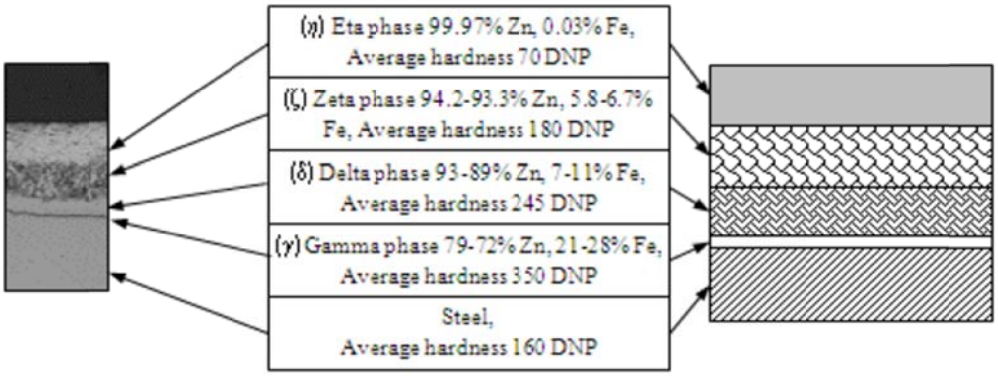

Figure 2.3. Cross-section of typical hot-dip galvanised zinc coating with relative proportions of different phases.[5]

If the content of silicon in the steel is not appropriate for the thickness of the zinc coating that is formed, it is not possible to achieve an exact thickness of the zinc coating by controlling the dipping time. The kinds and number of phases that the zinc

[1] Yeomans, S.R. (2004). *Galvanizing of Steel Reinforcement for Use in Building and Construction*.
[2] Esko Sistonen (2009). *Service Life of Hot-dip Galvanised Reinforcement Bars in Carbonated and Chloride-Contaminated Concrete*, p.17.
[3] Yeomans, S.R. (2004). *Galvanizing of Steel Reinforcement for Use in Building and Construction*.
[4] Galvanizers' Association of Australia (1999). *After-Fabrication Hot Dip Galvanizing*.
[5] Esko Sistonen (2009). *Service Life of Hot-dip Galvanised Reinforcement Bars in Carbonated and Chloride-Contaminated Concrete*, p.18.

includes depends on both the manufacturing process and the chemical composition of the steel. The zinc coating can be formed just in one phase. The variation in the microstructure of the zinc coating does not have much significance for the corrosion resistance. Actually, the most important property regarding corrosion in protection is the thickness of the zinc coating and, especially, the proportion of the eta (η) phase in the total thickness.[1] Moreover, the total thickness should be between 60 µm and 100 µm and the thickness of the eta (η) phase approximately 10 µm. The zinc coating can be formed homogenously and uniformly.[2]

2.3.1.1 Thickness and formation of zinc coating

The protective effect of the zinc coating is better as the zinc coating gets thicker. In addition, if the zinc coating is too high, it can create problems due to the reduction of the bond between the steel and the concrete.[3] Besides, cracks and spalls can appear on the zinc coating if the zinc coating thickness is too thick. Thus, the absolute maximum thickness of the zinc coating recommended is 200 µm.[4] Furthermore, a zinc coating with eta (η) offers notably stronger corrosion protection in concrete than a zinc coating with no eta (η).[5]

2.3.1.2 Factors influencing the thickness and formation of zinc coating

The thickness, the formation of the phases and the formation of the zinc coating depend, among other factors, on the bath temperature, the dipping time, the cooling rate, and the steel properties, especially the content of silicon in the steel. It is a complicated process. Usually it is possible to achieve all the phases with a normal temperature range [440-470ºC] and the rate of the steel-zinc reaction does not change remarkably. The dipping time is influenced by the shape and the thickness of the galvanised piece. The eta (η) phase may yet react with the steel and transform to zeta (ξ) phase if a piece lifted from the zinc bath cools slowly in air. Nevertheless, a variation of the microstructure is possible; which is influenced by the cooling rate. The cross sectional area of the piece determines the minimum thickness of the zinc layer.[6]

The formation of the zinc coating is influenced by the chemical composition of the steel. Reactive components of steel as silicon (Si) and phosphorus (P) can affect the quality of hot-dip galvanisation, although most of steels can be galvanised. Moreover, galvanisation conditions are significantly influence by the interaction of iron, zinc and

[1] Yeomans, S.R. (2004). *Galvanized Steel in Reinforced Concrete*.
[2] Andrade, C. et al. (1992). *Protection Systems for Reinforcement*.
[3] Andrade, C. et al. (1995). *Coating Protection for Reinforcement*.
[4] Andrade, C. et al. (1992). *Protection Systems for Reinforcement*.
[5] Maahn, E., Sorensen, B. (1996). *Influence of Microstructure on the Corrosion Properties of Hot-dip Galvanized Reinforcement in Concrete*.
[6] Marder, A.R. (2000). *The metallurgy of zinc-coated steel*.

silicon, such as the fact that molten zinc may react at the same rate as steel, although the zinc layer is growing.[1]

Hot-dip galvanised steel requires chemical factors for its coatings according to ASTM standard[2] (ASTM A385 - 2003) as: silicon below 0.04% or between 0.15% 0.22%, carbon below 0.25%, manganese below 1.3% and phosphorus below 0.04%. The most important element added to the hot-dip galvanising bath is presumably aluminium, which can develop different properties depending on its level content (usually used between 0.15% and 0.19%).[3] Thus, the inhibition layer may decompose with low aluminium additions.

2.3.2 Protection mechanisms of zinc coating

Zinc usually reacts with both strong alkalis and acids, it is an amphoteric metal. With pH values over 13 or below 6 the reaction of zinc is intensified. The corrosion of zinc is slow between pH values 6 and 13 due to the passive form of the surface of the zinc developed by corrosion products. The steel is protected by zinc in two forms. First, the steel surface is protected against aggressive materials from penetrating by zinc coating acting as barrier protection. In this case a durable passive layer is developed on the steel surface to have a protective action. However, the zinc may be damaged early if the passive layer does not develop. Moreover, the structure and thickness of the zinc coating have influence on the duration of the protective action of the zinc coating. Thus, the zinc coating can be damaged as a result of variations in the thickness of the original coating, non-uniform corrosion or high porosity (the steel is not protected by the coating). In this case, the uncoated steel is cathodically protected by the remaining zinc as the rate of corrosion of zinc increments. In this process *(Fig. 2.4)*, the dissolved zinc from the zinc coating moves to the cathode (steel without protection) and is deposited, thus it protects the steel. Firstly, the damaged area of steel is corroded but gradually light grey spots appear to cover the damaged area. Furthermore, the damaged areas that the zinc can protect cathodically are influenced by the conductivity of the electrolyte and by the thickness of the zinc coating.[4] Hence, local cracks (up to 3 mm wide) in the zinc coating of the steel can be protected and repaired by the zinc layer.[5]

[1] Esko Sistonen (2009). *Service Life of Hot-dip Galvanised Reinforcement Bars in Carbonated and Chloride-Contaminated Concrete*, p.19.
[2] ASTM A385 (2003). *Standard Practice for Providing High Quality Zinc Coatings*.
[3] Marder, A.R. (2000). *The Metallurgy of Zinc-coated Steel*.
[4] Esko Sistonen (2009). *Service Life of Hot-dip Galvanised Reinforcement Bars in Carbonated and Chloride-Contaminated Concrete*, p.23.
[5] Andrade, C. et al. (1992). *Protection Systems for Reinforcement*.

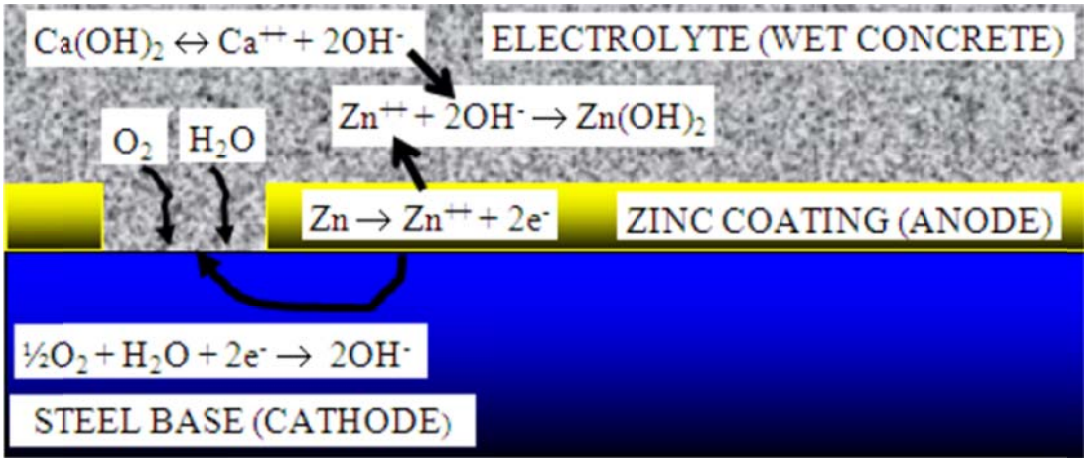

Figure 2.4. Cathodic protection of zinc coating in carbonated concrete.[1]

Figure 2.4 illustrates the reaction equations in cathodic protection. In chloride-contaminated concrete, zinc does not provide cathodic protection.[2] In this case, small anode related to a large cathode is formed and strong pitting corrosion may appear. The conductivity of the concrete electrolyte is, among others, a significant factor on the activity of the cathodic protection. Moreover in pitting corrosion, the rate of corrosion of the ordinary steel is higher than with galvanised. Besides, the effect of the autocatalytic mechanism for ordinary steel is slowed. In addition, in concrete containing chloride was not found cathodic protection and strong pitting corrosion appeared after the local corrosion of the zinc.[3] Generally, a zinc coating cannot act as active protector for steel when it is passive, furthermore the rate of corrosion does not diminish in unprotected areas. After the inhibition of zinc coating, the chloride content in the concrete is higher than the threshold value for ordinary steel and its rate of corrosion is very strong.

In addition, the ratio of the uncoated steel area to the zinc area is related with the rate of corrosion of zinc in sacrificial protection. Moreover, this rate of corrosion is proportional to the corrosion current per unit of zinc area, which is also related with the electrical conductivity of the electrolyte. The decisive factor in corrosion is not so much the electrical conductivity of the electrolyte as the quantity of the potential difference.[4]

2.3.2.1 The formation of the passive layer of the galvanised pipe

Before the concreting the passive layer of the galvanized pipe can be found if the pipe steel is chromatized (in a chromate bath) or oxidation of the galvanized pipe is adequate. Normally, it is possible to avoid the formation of white rust on galvanised products by chromatizing the piece, moreover it avoids the evolution of hydrogen

[1] Esko Sistonen (2009). *Service Life of Hot-dip Galvanised Reinforcement Bars in Carbonated and Chloride-Contaminated Concrete*, p.23.
[2] Andrade, C. et al. (1995). *Coating Protection for Reinforcement*.
[3] Nürnberger, U. (2000). *Supplementary Corrosion Protection of Reinforcing Steel*.
[4] Porter, F. (1991). *Zinc Handbook, Properties, Processing and Use in Design*.

between the zinc and the cement matrix, which may reduce the connexion of the concrete with the pipe. Chromatizing by lengthening the initiation time of active corrosion can increase the corrosion resistance of galvanised pipes.[1]

There are two different ways to chromatizing. The formation of a passive layer is generated by chromates of either concrete or pore water, or steel pipes can be chromatized in a chromate water bath (> 32 ºC). This point of view is appropriate when the chromate level is low and it is not desired to add this material to the concrete. Nowadays the use of chromates is not suitable, for health reasons.[2]

The composition of the chromate solution used, its pH value, the temperature, the quality of the coating, and the state of the surface are the factors to decide the thickness and protection properties of the zinc-steel layers.[3]

2.3.2.2 The corrosion resistance of galvanised steel in fresh concrete

The passivation phenomenon is the main factor on the corrosion resistance of steel. In this process, on the surface of the steel a hydroxide layer or tight oxide is formed. The corrosion current can be decreased substantially with a less dissolution of the metal, the passive layer may almost prevent it. The passive layer has a structure either amorphous (non-crystalline) or crystalline. Thus, crystalline structures develop a highly ordered repeating pattern and amorphous structures form a random orientation. Moreover, in the reaction produced between zinc and fresh concrete the most significant phases are the reaction of the zinc and calcium hydroxide, the evolution of hydrogen and the passivation of the zinc surfaces.[4]

In strongly alkaline concrete, the chemical equations of the corrosion of zinc are the following:[5]

Cathode reaction $2H_2O + 2e^- \rightarrow H_2\,(g) \uparrow + 2OH^-$,

Anode reaction $Zn\,(s) + 4OH^- \rightarrow Zn(OH)_4^{2-} + 2e^-$,

Total reaction $Zn\,(s) + 2OH^- + 2H_2O \rightarrow Zn(OH)_4^{2-} + H_2\,(g) \uparrow$.

Calcium hydroxozincate appears due to the immediate conversion of zinc[6]; thus, on the zinc surface, calcium hydroxozincate forms a barrier layer:[7]

---

[1] Esko Sistonen (2009). *Service Life of Hot-dip Galvanised Reinforcement Bars in Carbonated and Chloride-Contaminated Concrete*, p.24.
[2] Andrade, C. et al. (1992). *Protection Systems for Reinforcement*.
[3] Esko Sistonen (2009). *Service Life of Hot-dip Galvanised Reinforcement Bars in Carbonated and Chloride-Contaminated Concrete*, p.24.
[4] Esko Sistonen (2009). *Service Life of Hot-dip Galvanised Reinforcement Bars in Carbonated and Chloride-Contaminated Concrete*, p.26-27.
[5] Vinka, T.-G., Becker, M. (1998). *Corrosion of Galvanised Steel in Concrete*.
[6] Yeomans, S.R. (1987). *Galvanized Steel Reinforcement in Concrete*.
[7] Andrade, C. et al. (1995). *Coating Protection for Reinforcement*.

$2Zn + Ca(OH)_2 + 6H_2O \rightarrow Ca[Zn(OH)_3]_2 \cdot 2H_2O + 2H_2 \uparrow$.

Moreover, the liberation of hydrogen gas in concrete and formation of dissolved zincate is probable:[1]

$Zn + 2OH^- \rightarrow ZnO_2^{2-} + H_2 \uparrow$.

Zinc hydroxide is formed due to the fact that zincate reacts with water. Moreover, zinc hydroxide is slightly soluble in water:

$ZnO_2^{2-} + 2H_2O \rightarrow Zn(OH)_2 + 2OH^-$.

The pH value and the composition of the fresh concrete are factors that affect the type and stability of the reaction products that are formed in the corrosion reaction. Right after curing, the pH value of concrete (12-14) is high, determined by the hydration rate and composition of the cement. Moreover, calcium hydroxide is developed in the hydration of the cement and the alkalinity is influenced by sodium salts and freely soluble potassium.[2] The pore water of concrete is saturated with $Ca(OH)_2$ (pH 12.6) for a short period after the mix of cement and water. Few days later substances as NaOH and KOH keep (maintain) the high pH value because of their high solubility. In early stages of the hydration when is typical a slightly lower pH, the solution becomes saturated with Ca^{2+} - ions. For developing the passive zinc layer in alkaline material the presence of calcium ions is essential.[3]

In addition, calcium hydroxide is used in the next phases of hydration of the silica cement and the pH of the hardened concrete reduces. Moreover, fly ash cement and blast-furnace slag have not a high influence. However, Andersson et al. determined for a Portland cement concrete the pH (13.4) was the same as for a pore solution of fly ash concrete, ten months later of its exposure (but the calcium content was only one sixth).[4] Besides, zinc is transferred to the passive area when the value of the pH decreases after curing, although the formation of the passive layer is imperilled due to the reduced calcium hydroxide content. Nevertheless, the hydrogen evolution is reduced due to lower pH value and low water-to-binder ratio.[5]

The formation of the passive layer depends significantly on the size of the zincate crystals.

The size of the crystals increases when the pH value rises, corrosion products appear above a pH value of 13.2 ±0.1[6] as single crystals which do not cover the surface due to

[1] Sarja, A. et al. (1984). *Zinc-coated Concrete Reinforcement*.
[2] Esko Sistonen (2009). *Service Life of Hot-dip Galvanised Reinforcement Bars in Carbonated and Chloride-Contaminated Concrete*, p.27.
[3] Alonso, C. et al. (2000). *The Addition of Ni to Improve the Corrosion Resistance of Galvanized Reinforcement.*
[4] Andersson, K. et al. (1989). *Chemical Composition of Cement Pore Solutions*.
[5] Fagerlund, G. (1990), *Durability of Concrete Structures, Summary Review*.
[6] Andrade, C. et al. (1995). *Coating Protection for Reinforcement*.

the fact that the concentration of Ca^{2+} - ions in solution is reduced at pH values above 13.2. The zinc continues to actively corrode and may completely dissolve in a short period of time because the zinc surface does not passive due to the lack of Ca^{2+} - ions.[1] For the durability of zinc coating is primary lower pH value of concrete under 13.2. Alonso et al. found that the hydrogen evolution and zinc reactivity are reduced if nickel is added to the zinc bath in alkaline conditions. Thus, the zincate crystals can cover and protect the zinc coating due to their smaller size. Moreover, the stability of a passive layer of calcium hydroxozincate $Ca(Zn(OH)_3)_2 \cdot 2H_2O$ does not change any more if pH later rises.[2] Nevertheless, several factors influence the zinc passivation process giving rise to complicated reactions difficult to understand.

Compared to the rate in low-alkali cement the rate of corrosion of hot-dip galvanised pipes in high-alkali cement can be as much as over tenfold.[3] The pH value increases from 12 to 14 as the rate of corrosion changes exponentially. The rate of corrosion increases significantly above a pH value for concrete of 13.[4] Andrade et al found that if the cement applied is low-alkaline, a tight and uniform layer forms on the surface of the galvanised steel. As the concrete hardens, the reactions between the alkaline concrete and zinc are finished. However, the formation of the passive layer is not indicative for the halting of the reaction. Furthermore, the formation of the passive layer is prevented due to the presence of chlorides in the fresh concrete. The zinc is less stable at higher pH values. Thus, the initiation of corrosion will be possible with lower chloride content when the pH is high.[5]

2.3.2.3 Influence of hydrogen evolution

In porous concrete carbonation and detrimental substances such as water, oxygen, and chlorides are highly propagated. However, the corrosion products of zinc are able to expand into the hydrogen pores. In the absence of an eta (η) phase, the rate of corrosion of the zinc is also higher. Alonso et al. shown that after the contact between the alkaline matter and the zinc the development of hydrogen begins soon.[6] The reaction of a zinc-iron alloy (mainly zeta (ξ) phase) surface form more easily hydrogen gas than with eta (η) phase. In the absence of an eta (η) phase, the rate of corrosion of the zinc is also higher.[7] Furthermore, the nonexistence of an eta (η) phase does not have any importance with respect to the rate of corrosion and the reaction leading to the evolution of hydrogen is stopped if the zinc surface has oxidised before concreting or hot-dip galvanised pieces are chromatized.[8]

---

[1] Andrade, et al. (2004). *Electrochemical Aspects of Galvanized Reinforcement Corrosion*.
[2] Alonso, C. et al. (2000). *The Addition of Ni to Improve the Corrosion Resistance of Galvanized Reinforcement.*
[3] Andrade, C. et al. (1995). *Coating Protection for Reinforcement*.
[4] Andrade. C. et al. (1983). *Relation between the Alkali Content of Cements and the Corrosion Rates of the Galvanized Reinforcements*.
[5] Andrade, C. et al. (1995). *Coating Protection for Reinforcement*.
[6] Alonso, C. et al. (2000). *The Addition of Ni to Improve the Corrosion Resistance of Galvanized Reinforcement.*
[7] Vinka, T.-G., Becker, M. (1998). *Corrosion of Galvanised Steel in Concrete*.
[8] Yeomans, S.R. (1993). *Coated Steel Reinforcement in Concrete*.

In concrete, chromates act as inhibitors.[1] Corderoy et al. confirmed that as the chromate ions reduce, the formation of hydrogen stops almost totally, instead of the water. Chromium oxide (Cr_2O_3) is formed from chromium trioxide (CrO_3) with a pH value of nearly 12.5. In this case, chromium oxide, zinc chromate and maybe zinc hydroxide form a passive layer (the reaction is not precisely known). Several factors regarding the durability of a water-soluble chromate layer after cleansing, storage, installation exposed to rain and transport are very uncertain.[2] Besides, Yeomans stated that the long time (more than some weeks or months) durability of the chromate layer of galvanised steel cannot be guaranteed. Hence, chromatized steel should be used as soon as possible after chromatizing due to their low durability and water-solubility.[3,4]

Moreover, the organic acids are easily devastated. Hence, a salt film on the surface of the zinc is formed due to the passivation effect of organic acids via atmospheric passivation. In the galvanisation process hydrochloric and sulphuric are already used. Then it is possible to use these acids in the passivation of the zinc coating and preventing the evolution of hydrogen.[5]

The evolution of hydrogen along the surface of the pipe is caused simultaneously by corrosion and passivation in galvanised steel. Severe hydrogen evolution takes places as soon as a zinc coating is subjected to contact with alkaline media. But, when the CaHZn layer forms, it decreased uniformly. Usually the time during which hydrogen evolves is around 1-2 hours in circumstances without chlorides. The duration of the evolution of the hydrogen may be several hours long in chloride-contaminated circumstances. Anyway, it depends primarily on the chromium and alkali content of the cement.[6]

The level of corrosion of zinc in fresh concrete could be reduced with suitable concrete properties as the amount of hydrogen evolving.[7]

Adding silica, fly ash, or blast furnace slag as blend components can reduce the pH of concrete. The formation of the passive layer may abort as the amount of free calcium hydroxide decreases, when these components are used.[8]

Furthermore, by proper selection of materials the evolution of hydrogen and the porosity caused by it can be reduced, so that the final result could be acceptable. Moreover, the pH value, the water-to-binder ratio, compactness, the amount of free calcium hydroxide, ductility, differences in alkalinity between different cement types

[1] Andrade, C. et al. (1995). *Coating Protection for Reinforcement*.
[2] Corderoy, D.J.H., Herzog, H. (1978). *Passivation of Galvanized Reinforcement by Inhibitor Anions*.
[3] Yeomans, S.R. (1987*). Galvanized Steel Reinforcement in Concrete*.
[4] Yeomans, S.R. (1993). *Coated Steel Reinforcement in Concrete*.
[5] Esko Sistonen (2009). *Service Life of Hot-dip Galvanised Reinforcement Bars in Carbonated and Chloride-Contaminated Concrete*, p.29.
[6] Yeomans, S.R. (2004). *Galvanized Steel in Reinforced Concrete*.
[7] Esko Sistonen (2009). *Service Life of Hot-dip Galvanised Reinforcement Bars in Carbonated and Chloride-Contaminated Concrete*, p.30.
[8] Arliguie, G. (2001). *Performance of Galvanized Rebar*.

and binder, among other properties of concrete have a significant effect on the porosity and hydrogen evolution. In addition, with the goal to shorten the time for the hydrogen evolution and zinc reaction the use of rapid-hardening cements and low-alkaline concretes is recommended.[1]

2.3.2.4 Zinc in hardened concrete

On the surface of ordinary steel, a corrosion protected oxide layer is formed as a result of the alkalinity of the concrete. However, due to the carbonation of the concrete or chloride attack, the layer disappears. The ordinary steel and the galvanized steel are protected by the concrete cover from the damaging effects of air contamination. In addition, the pH value decreases to approximately 8.0-8.5 from approximately 12.5-14.0, in the concrete carbonates due to the action of carbon dioxide. Thus, if the other corrosion conditions are satisfied, the corrosion of ordinary steel becomes possible when the pH value of the concrete is reduced down to 11.5.[2]

Furthermore, in carbonated concrete, the ordinary steel is less durable than zinc-coated steel due to the fact that through a much wider pH range zinc is passive, approximately up to a pH value of 9.5 for the concrete.[3] The zinc continues corroding till the concrete is nearly carbonated to the level of the steel. Moreover, the fact that a variable concrete quality and a possible reduced cover thickness due to poor workmanship is more dangerous for the concrete with ordinary steel than that with the zinc-coated steel.[4] However, the porous layer (formed by the hydrogen bubbles) makes it easier for detrimental material and carbon dioxide to ingress to the level of the steel if the passivation process of the zinc coating fails. In this case, the active corrosion process could appear early. Nevertheless, if the thickness of the concrete cover is compared with the thickness of the porous layer, the latter may be insignificant.[5]

2.3.3 Corrosion measurements

With measurements of the corrosion current, corrosion potential and the resistivity of the concrete it is possible to estimate the state of corrosion. The corrosion current (I_{corr}) and corrosion potential (E_{corr}) have a correspondence with a notable difference between diverse research data.[6] This correlation can also be found between the resistivity of concrete (R_c) and the corrosion potential (E_{corr}), and between the resistivity of concrete (R_c) and the corrosion current (I_{corr}). The rate of corrosion of zinc

[1] Esko Sistonen (2009). *Service Life of Hot-dip Galvanised Reinforcement Bars in Carbonated and Chloride-Contaminated Concrete*, p.31.
[2] Esko Sistonen (2009). *Service Life of Hot-dip Galvanised Reinforcement Bars in Carbonated and Chloride-Contaminated Concrete*, p.31.
[3] Yeomans, S.R. (1993). *Coated Steel Reinforcement in Concrete*.
[4] Andrade, C. et al. (1995). *Coating Protection for Reinforcement*.
[5] Esko Sistonen (2009). *Service Life of Hot-dip Galvanised Reinforcement Bars in Carbonated and Chloride-Contaminated Concrete*, p.31.
[6] Andrade, C., Alonso, C. (2001). *On-Site Measurements of Corrosion Rate of Reinforcements.*

(eta (η) phase) v_{corr} [µm/year] can be obtained from the corrosion current of zinc (eta (η) phase) I_{corr} [µA/cm^2], according to Faraday's law and the density of zinc, as follows:

1 µA/cm^2 = 15.0 µm/year *(Equation 2.1)*

With the eta (η) phase this factor is higher than with iron-zinc alloy *(Equation 2.1)*. Thus, a rate of corrosion of 11.6 µm/year is corresponded to a corrosion current of 1 µA/cm^2 with ordinary steel. The *Table 2.1* illustrates the correlation between the corrosion current and the state of corrosion. The moisture content and pore structure of the concrete affects, among other factors, the resistivity of the concrete. The resistivity of water saturated concrete has been measured around 10 kΩcm and of dry concrete up to 10^6 kΩcm. In the case of dry concrete, there is no sufficient electrolyte needed for corrosion.[1] Thus, when the steel is actively corroding, the approximate rate of corrosion and the conditions for possible corrosion are related with the values of the resistivity of concrete (Rc) and the state of the moisture content in concrete. The possible state of corrosion and the range of resistivity of the concrete are illustrated in *Table 2.2*.

Corrosion current [µA/cm^2]	Rate of corrosion of zinc coating [µm/a]	State of corrosion
< 0.1	< 1.5	Passive
0.1 – 0.5	1.5 – 7.5	Low
0.5 – 1	7.5 – 15	Moderate
> 1	> 15	High

Table 2-1. State of corrosion based on corrosion current measured in laboratory and field conditions.[2] (a = year)

Resistivity of concrete [kΩcm]	State of corrosion
> 100 – 200	Cannot distinguish between active and passive steel
50 – 100	Low rate of corrosion
10 – 50	Moderate to high rate of corrosion where steel is active
< 10	Resistivity is not the controlling parameter (Severe)

Table 2-2. The range of resistivity of the concrete and the possible state of corrosion with normal portland and blended cement.[3]

Moreover, the potential difference between the electrolyte and the surface of the ductile-iron pipe (zinc in this case) can be considered as the corrosion potential expressed in mV. Thus, the potential difference between a reference electrode in contact with the ductile-iron and the electrolyte is measured due to the fact that the corrosion potential cannot be measured in practice. Hence, the potential difference

[1] Locke, C.E. (1986). *Corrosion of Steel in Portland Cement Concrete: Fundamental Studies.*
[2] Andrade, C., Alonso, C. (2001). *On-Site Measurements of Corrosion Rate of Reinforcements*.
[3] Andrade, C., Alonso, C. (2001). *On-Site Measurements of Corrosion Rate of Reinforcements.*

between the concrete and the ductile-iron can be calculated, when the potential of the reference electrode is known and stable.[1]

2.4 Corrosion resistance of ductile-iron pipe

Cast iron pipes were extensively used to build water distribution systems from the early 1900s until ductile iron pipes were introduced in the 1970s.

Cast-iron pipe has been succeeded by ductile-iron pipe due to its substantially improved structural properties and its higher strength.[2] Moreover, other important properties of grey cast iron as ease of casting, corrosion resistance, economy and easy for installation are also processed by ductile-iron pipe. Besides, carbon content provides both cast iron and ductile iron better corrosion resistance for the metals. Thus, carbon in grey cast iron usually is dispersed throughout the metal matrix, in the form of interlocking flakes of graphite. Moreover, the graphite takes the form of spheroids or nodules due to an added stage in the processing of the molten metal during the production process in ductile iron. When corrosion of both materials appears, the corrosion products will add graphite present and they may adhere firmly to the metal substrate without damage. Hence, a further corrosion attack can be slowed or even stopped in many soil environments due to the barrier previously formed by the graphite coating. Furthermore, many pipelines without protect coating in corrosive environments may have long service life due to the protective effect of graphite corrosion by-products, which have significant mechanical strength.[3]

Several studies have been developed for evaluating the resistance against corrosion of the ductile-iron pipe. The corrosion resistance of the ductile-iron pipe was at least as good as that of grey iron pipe according to the studies with a preserved interpretation of the data.[4,5] Moreover, a little difference in chemical compositions exists between both materials; the ductile-iron graphite is formed of spheroidal shape giving rise a fundamental advantage respect to corrosion resistance over grey iron.[6] The graphite surface can act as cathode to protect the iron from anodic corrosion and this has better behaviour when the graphite is in the form of spheres rather than flakes. Thus, pitting corrosion is stronger in grey iron due to the fact that the interlock flakes of graphite performance a higher depth of penetration. Consequently, after several studies and analysis of data, ductile iron pipe had exposed for longer periods and the existence of this advantage and conclusions regarding the corrosion resistance of

[1] Camitz, G., Pettersson, K. (1989). *Corrosion Protection of Steel in Concrete - Stage 1, Cathodic Corrosion Protection of Steel Reinforcement in Concrete* - The Literature Review.
[2] Ductile Iron Pipe Research Association (1984). *Handbook of Ductile Iron Pipe*. Birmingham, Ala.
[3] Ductile Iron Pipe Research Association*. Cast Iron Pipe Century Club Records*. Birmingham, Ala.
[4] Cast Iron Pipe Research Association (1964). *Soil Corrosion Test Report: Ductile Iron Pipe.*
[5] Sears, E.C. (1968). *Comparison of the Soil Corrosion Resistance of Ductile Iron Pipe and Gray Cast Iron Pipe. Materials Protection*, 7(10):33-36.
[6] Laque, F.R. (1964). *Corrosion Characteristics of Ductile Iron*. Jour. AWWA, 56(11): 1433.

ductile-iron pipe were confirmed.[1] Besides, the ductile iron develops a spheroidal graphite structure giving rise to corrosion attack extended out by whole the surface of the metal; then this process occurs more than in grey iron, which usually support pitting corrosion. In brief, grey-iron pipe is more susceptible than ductile-iron pipe against pitting corrosion, which is a factor to evaluate the resistance of the pipe to failure by perforation, leading to leakage of water.[2]

Moreover, another important factor is the length of the pipe; usually the ductile-iron pipe is manufactured in 5 m and 6 m, and uses a rubber-gasketed jointing system. Thus, ductile-iron pipelines are recognised to be electrically discontinuous due to the fact that the joints give resistance of sufficient magnitude. Consequently, long line corrosion current is more difficult to develop. Thus, except in situations where the electrical continuity is necessary for cathodic protection and corrosion control, joint bonding of ductile-iron pipelines is usually discouraged.[3]

2.5 Concrete cover for ductile-iron pipe

Concrete is mostly used as construction materials. However, concrete is also utilized on steel surface as corrosion resistant coatings. Thus, when the concrete is well proportioned, it is a good corrosion resistant coating convenient for steel. It supplies a dense, thick, hard and water-resistant barrier, which produces an environment to inhibit the corrosion of steel.[4]

Furthermore, a lot of water pipelines are covered with concrete, both cast iron and ductile iron with cement mortar coating. Thus, concrete coating for water pipe has preserved its characteristics and has protected iron from corrosion processes for more than 100 years (likely, one of the most durable coating). When the concrete is exposed to fresh water and the atmosphere, it provides the best protection.

Another important property of concrete is its hardness. It has good properties against abrasion. Besides, concrete has good compressive strength, which is its most important property.

As time passes, the concrete improves several properties. The hardness of the concrete and compressive strength can improved when it is under water over a long time due to long-term slow hydration. Moreover, concrete increases its hardness and compressive strength due to the reaction between lime and carbon dioxide from the air to form calcium carbonate. In summary, concrete is a durable material under most usual environmental situations. Nevertheless, under chemical exposures (essentially

[1] Fuller, A.G. 1981. *Corrosion Resistance of Ductile Iron Pipe*. BCIRA Report 1442. Alvechurch, Birmingham: BCIRA.
[2] American Water Works Association (AWWA), (2009). *Ductile-Iron Pipe and Fittings - Manual of Water Supply Practices, M41. (3rd Edition)*, p. 172.
[3] American Water Works Association (AWWA), (2009). *Ductile-Iron Pipe and Fittings - Manual of Water Supply Practices, M41. (3rd Edition)*, p. 173.
[4] Lichtenstein, Joram (2002). *Coatings for concrete and concrete pipe*. Materials Performance, p.66.

acidic ones) the concrete is a very reactive material. Actually, in some cases, the concrete will be dissolved by pure flowing water. Because concrete is also a reactive material, to stop or to retard the corrosion (and contamination of chemical solution), it is indispensable to separate the concrete from other reactive materials. [1]

2.6 Epoxy coating for ductile-iron pipe

The external coatings for pipes have been derived from other materials as bituminous products, giving rise to epoxy coatings. A combination of a durable, resistant and effective coating and cathodic protection are required to prevent the corrosion for underground pipelines. The resistivity of the coating used on a pipe has influence with the cathodic protection. The electrical characteristics of the coating and the total area of exposed steel, as a result of damage to the coating, are related to the resistivity of the area. The factors of the environment as soil resistivity, temperature and coating system have an influence on the effectiveness of the protection.[2]

One of the more commonly used pipeline coating is the single-layer FBE (Fusion Bonded Epoxy), since 1960 when it was introduced. Single-layer FBE capacity has proven as a pipeline coating. The epoxy also has proven performance in underground and undersea service, among other characteristics to the application and the construction processes. For pipes, girthwelds, fittings and bends, the epoxy coating has proven effective. Moreover, it works effectively with impinged concrete, directional-bore installation, and high pipeline operating temperatures, when a greater thickness is used.[3]

Thus, the epoxy as pipe coating has good properties as the following characteristics:[4]

- Excellent adhesion to many substrates.
- Good chemical resistance.
- Low oxygen permeability.
- Non-shielding - works with zinc coating cathodic protection.
- No reported cases of stress-corrosion cracking (SCC) of pipe coated with FBE. [5]
    - The coating remains bonded to the extent that it separates the pipeline steel from an SCC chemical environment.
    - It allows the passage of current in case of bond failure.

---

[1] Lichtenstein, Joram (2002). *Coatings for concrete and concrete pipe*. Materials Performance, p.66.
[2] R. L. Bianchetti, "Economics," A. W. Peabody, R. L. Bianchetti, eds. (2001), *Control of Pipeline Corrosion*, 2nd ed., (Houston, TX: NACE, 2001), p. 295.
[3] Kehr, A, Dabiri, M, Hislop, R*, (2003). Dual-Layer Fusion-Bonded Epoxy (FBE) Coatings Protect Pipelines*, BHR Group, 15th International Conference on Pipeline Protection, October 29-31, 2003, Aachen, Germany. pp. 2.
[4] Kehr, A, Dabiri, M, Hislop, R*, (2003). Dual-Layer Fusion-Bonded Epoxy (FBE) Coatings Protect Pipelines*, BHR Group, 15th International Conference on Pipeline Protection, October 29-31, 2003, Aachen, Germany. pp. 2-3.
[5] J. Banach, (1997). *FBE: An End-User's Perspective*, NACE TechEdge Program, Using Fusion Bonded Powder Coating in the Pipeline Industry, Houston, June 1997.

        - The cleaning process alters the surface to make it less susceptible to SCC (removes mill scale and induces stress through blast cleaning).[1]
        - FBE is one of the high-performance coatings that meet these requirements.
- Resistance to biological attack.
- Tough – frequently installed under the sea, through rolling plains, in rocky, mountainous areas, in the desert, and the arctic.
    - Excellent penetration resistance.
    - Good impact resistance.
        - Impact damage is limited to the point of contact.
        - Damage is easily seen.
        - Damage is easily repaired.
    - Good abrasion resistance.
    - Good flexibility.

[1] G. H. Koch, T. J. Barlo, W. E. Berry, "Effect of Grit Blasting on the Stress Corrosion Cracking Behavior of Line Pipe Steel," MP, Vol. 23, No. 10, October 1984, pp. 20 – 23.

3 EVALUATION OF CORROSIVE SOILS

3.1 Soil properties in general

Structures in buried conditions present challenges due to the heterogenity and different characteristics of the soils. The variability of parameters as moisture, salts and organic materials modifies the electrolyte conditions giving rise to challenges in the corrosivity conditions present in buried pipelines.

Moreover, the composition of the soil has an influence on the corrosion conditions and variability. Thus, granular soils as gravel, sand, loam or chalk usually have high resistivity and they are dry and aired. Generally, this kind of soil may not be aggressive according to corrosion conditions. On the contrary, soils as morbs, humus without lime or organic materials (usually acid) are highly aggressive. In an intermediate point, clay can be sometimes aggressive, because it is habitually wet and conductive.[1]

Besides, several procedures to analyse and evaluate the soils according to corrosivity can be found for ductile-iron pipes. Different examples are the next ones: the numeric scale AWWA C-105 (*Table 3.1*) and DVGW-GW9 (*Table 3.2*) with common parameters as resistivity, moisture, pH, Redox potential and sulfide content.

Soil-test evaluation for gray or ductile cast-iron pipe (10-point system)*

Soil Characteristics		Points
Resistivity Ω-cm†	<1,500	10
	≥1,500–1,800	8
	>1,800–2,100	5
	>2,100–2,500	2
	>2,500–3,000	1
	>3,000	0
pH	0–2	5
	2–4	3
	4–6.5	0
	6.5–7.5	0‡
	7.5–8.5	0
	>8.5	3
Redox potential	> +100 mV	0
	+50 to +100 mV	3.5
	0 to +50 mV	4
	Negative	5
Sulfides	Positive	3.5
	Trace	2
	Negative	0
Moisture	Poor drainage, continuously wet	2
	Fair drainage, generally moist	1
	Good drainage, generally dry	0

* Ten points—corrosive to gray or ductile cast-iron pipe, protection is indicated.

† Based on water-saturated soil box.

‡ If sulfides are present and low or negative redox-potential results are obtained, three points shall be given for this range.

Table 3-3. Soil test evaluation for grey or ductile-iron cast pipe (10-point system).[2]

[1] Franky Esteban Bedoya Lora (2010). *Corrosion en Suelos*. Colombia

[2] American Water Works Association. *Standard for Polyethylene Encasement for Ductile-Iron Pipe Systems. ANSI/ AWWA C105/A21.5.* Denver, Colo.

Item	*Measured Value*	*Marks*
Soil composition	Calcareous, marly limestone Sandy marl, not stratified sand	+2
	Loam, sandy loam (loam content 75% or less) marly loam, sandy claysoil (silt content 75% or less)	0
	Clay, marly clay, humus,	−2
	Peat, thick loam, marshy soil	−4
Ground-water level at buried position	None	0
	Exist	−1
	Vary	−2
Resistivity	10,000 ohm. cm or more	0
	10,000–5,000	−1
	5,000–2,300	−2
	2,300–1,000	−3
	1,000 or less	−4
Moisture content	20% or less	0
	20% or more	−1
pH	6 or more	0
	6 or less	−2
Sulphide and hydrogen sulphide	None	0
	Trace	−2
	Exist	−4
Carbonate	5% or more	+2
	5–1	+1
	1 or less	0
Chloride	100 mg/kg or less	0
	100 mg/kg more	−1
Sulphate	200 mg/kg or less	0
	200–500	−1
	500–1,000	−2
	1,000 or more	−3
Cinder and coke	None	0
	Exist	−4

Soil is regarded as non-corrosive if the total of the above is 0 or higher; Slightly corrosive if 0 to −4; corrosive if −5 to −10 and very corrosive if −10 or less.

Table 3-2. Soil test evaluation numeric scale German Gas and Water Works Enginners Association Standard (DVGW GW9).[1]

Therefore, the resistivity (the reciprocal conductivity) is the factor with higher weight on the majority of classifications. The resistivity value depends among other factors on the soil structure, particle size, porosity, permeability, ion content and water content.

Usually, a soil with low resistivity will serve as an electrolyte as well. In this case, the corrosion of a structure may be high, but just for steels without any kind of cathodic protection. Moreover, steel or iron with protection, as zinc coating, may be less susceptible to low resistivity due to the fact that the cathodic protection is more effectively in this conditions.[2]

Furthermore, the resistivity can vary depending on the year state due to the changes of the water contents on the soil.

[1] DVGW GW 9:2011 (2011). *Evaluation Of Soils In View Of Their Corrosion Behaviour Towards Buried Pipelines And Vessels Of Non-Alloyed Iron Materials*

[2] Franky Esteban Bedoya Lora (2010). *Corrosion en Suelos*. Colombia

In addition, highly acid soils with pH < 5 can act as electrolyte and a high corrosion of the naked steel or iron may happen, so the soil aggressively increases with the acidity. For pH values between 5 and 8, corrosion depends on other factors and the soil supports sulfate-reducing bacteria if other conditions are suitable. The basic soils with pH > 8.5 are generally high in dissolved salt and usually exhibit low resistivity giving rise to risk corrosion.

Hence, considering only resistivity and pH parameter, galvanic structures may have longer service life for higher pH and resistivity.

The Redox potential is an indicator of the oxidate and reductive capacity of the soil. The sulfate-reducing bacteria are the most common one and it can be found in anaerobic conditions. Thus, a sufficient aired soil will not support sulfate reducers (Redox potential > 100 mV). A Redox potential between 0 mV and 100 mV may or may not show anaerobic conditions. Nevertheless, the Redox potential can be negative for anaerobic conditions under sulfate reducers.

Furthermore, the water content depends on the porosity and climate among other factors. In highly wet soils, a thin film of water is formed above the steel surface, giving rise to the oxygen transfer from the atmosphere. In this case, the anodic reaction is depolarized. In dry soils, corrosion tends to be null or minimal due to the anodic control. The soils present variation of moisture may be aggressive. Moreover, with a moisture content between >0% and 20%, the soil can be aggressive by pitting corrosion due to differential aeration, generating oxygen gradients and facilitating the formation of a pile on the soil.

Another important parameter affecting the possible corrosion is the content of anions, which has a significant influence on the resistivity. With more salt content a soil may be more conductive and it may have less resistivity. In another way, the calcium and magnesium have the contrary effect, they are deposited on the steel surface. Furthermore, the chloride ions and sulfides accelerate the corrosion due to the fact that they can break the passive layer locally. In addition, pitting corrosion can appear in presence of chloride or sulfate-reducing bacteria.

Usually, uniform corrosion is produced in homogeneous conditions of the soil and steel or iron surface; for heterogeneous conditions on the soil steel or iron surface the localized corrosion is easier.

On highly corrosive soils, the corrosion appears through micropiles generated by heterogeneous conditions on the steel surface or environment. The micropiles produce uniform corrosion throughout the steel surface and it may not be strong or severe. Moreover, structures formed by different metals, united physically and buried, may form galvanic cell.

Usually, in anaerobic conditions the microbiologic corrosion is developed. In this case, the sulfate-reducing bacteria generate sulfuric acids and sulfide from sulfate. These corrosion products damage the iron, cooper and lead among others.

Besides, on buried pipelines the pitting corrosion is typical parallel with uniform corrosion. The pitting corrosion can be produced due to local failures on the coating of the steel or iron, local phenomenon of differential aeration and the effect of aggressive anions as chloride, close to the sea.[1]

3.2 Swedish soil properties

In short, the soil of Sweden is basically formed of moraine, with almost a 75% of its extension. The other 25% is formed of a 10% of naked rock and the rest 15% of glaciofluvial deposits, fine grain and peat.[2]

These soils are composed of properties that are important for the corrosion process, both physically and chemically. The conditions of the Swedish soils have effects, both positively and negatively, in corrosion risk on metallic structures. There are highly solid soils or sands with rock shallow, then the formation of piles are limited. Usually, the phreatic level is shallow, then a lot of pipes are submerged. In the other hand, the Swedish soil, especially clays with high water content, has a high sulfide content and low carbonate content; it can produce corrosion.[3]

Moreover, the oxygen diffusion and moisture affect directly the rate of corrosion. These conditions are influenced by the water permeability on the ground and the proximity of the phreatic level or aquifer, although the variation of the underground water can influence due to the increase of the oxygen circulation. The rate of corrosion can be affected by low resistivity, increasing the corrosion, and by high salt content, as the west coast where salted water is contained on the soil.

Furthermore, a high pH, as in calcareous soils, ash and graphite decreases the rate of corrosion. In addition, on the installation phase of buried pipes, the ground is mixed with residues as ash, slag and with other soils of their environment. This process increases the rate of corrosion.

Besides, corrosion is higher if the soil has high permeability as rock or gravel close to open waters, where the water can flow through the pores; the rate of corrosion increases due to high content of oxygenated water. In addition, the presence of stone blocks can have negative effect if these blocks interrupt the protection of a layer.

[1] Franky Esteban Bedoya Lora (2010). *Corrosion en Suelos*. Colombia
[2] Göran Camitz, Ulf Bergdahl, Tor-Gunnar Vinka (2009). *Stalpalars beständighet mot corrosion i jord. En sammanställning av kunskaper och erfarenheter.*
[3] Göran Camitz, Ulf Bergdahl, Tor-Gunnar Vinka (2009). *Stalpalars beständighet mot corrosion i jord. En sammanställning av kunskaper och erfarenheter.*

Since 1983 Korrosioninstutet (KIMAB) has carried out several studies to check the corrosion in different steel states between several soils of Sweden.[1] Thus, some references about the Göteborg soil were concluded:

- Göteborg soil presented the highest rate of corrosion for ordinary steel (1.6 – 6 μm).

- Göteborg soil presented the 4th highest rate of corrosion for zincked steel (0.8 – 1.9 μm).

- The zinc may protect the iron and steel from corrosion under Göteborg soil, which is highly corrosive for naked steel.

3.3 Concluding Remarks

According to the conclusions taken from Korrosioninstutet (KIMAB) studies (Chapter 3.2 - "Swedish soil properties") the ductile iron pipes may have good behaviour against corrosion in Göteborg soils and normal service life when the zinc covers throughout the ductile-iron surface. However, when the zinc layer starts to inhibit, the corrosion risk is high in Göteborg soils. Thus, it would be recommendable to control this possible damage during the service life of the pipe.

Moreover, for the studied pipes, under Göteborg soils conditions, pitting corrosion could occur due to the chloride ions presence in Göteborg (close to the sea) and the possible damaged zinc in both specimens after impact energies > 180 J and with several cracks (sanding) on the surface.

[1] Göran Camitz, Ulf Bergdahl, Tor-Gunnar Vinka (2009). *Stalpalars beständighet mot corrosion i jord. En sammanställning av kunskaper och erfarenheter.*

4 EXPERIMENTAL WORK

To develop the investigation, it was decided to do the impact test according to ZM-U Fabrikstest (7.2.3 SS-EN 15542:2008) to simulate possible mechanical damage produced at different levels of impact energy, so as to be able to evaluate the effect of a possible impact under the installation phase of the pipes on the durability of the pipes with regard to iron corrosion. Afterwards, it was decided to develop a test in which the pipe specimens were dipped in a salt solution bath (NaCl 5%), which immersed ¾ of the pipe. In this test it was expected to accelerate the corrosion by applying an external electrical field, but it was proven difficult because a very low potential difference could result in a very high current due to very low ohmic resistance. Later, it was tried to monitor the open circuit potential, but the process was slow for getting significant potential changes in a short time. Therefore, this potential monitoring would not give distinguishing information about damage and corrosion. Thus the approach to the service life of the Zn-Fe was changed to the measurement of the potential (V) difference between different points of the surface and iron ductile. Later, the current passing through different parts of the pipe surface, with particular attention to the impact area, was measured by applying different potentials. This results in the estimation of resistance.

The pipes supplied by Göteborg Vatten were used in all the tests. 12 samples of 0.5 meters VRS-ZM class of 150 mm diameter and 7 samples of 0.6 meters of the same class with an epoxy coating, but without concrete cover, were prepared.

4.1 Impact test

To simulate the damage produced by an impact under the installation phase it was decided to apply the impact test according to ZM-U Fabrikstest (7.2.3 SS-EN 15542:2008). In which, the impact effect was simulated by dropping a weight on the coating with a given energy and checking the level of damage. The specimen was supported in such a way that the spring action of the specimen caused by the impact of the falling weight was absorbed. The impacting surface of the falling weight is a section of a hardened steel ball with a diameter of 25 mm.

The test was carried out at an ambient temperature. The height of the falling weight was in steps, approximately 1 m, 2 m and 3 m.

Care was taken to ensure that the impact energy was maintained at a constant level by step, ensuring that little or no friction was encountered when the falling weight was dropped.

The impact energy applied was 15 J per mm of nominal coating thickness as a standard. The VRS-ZM have a thickness of the concrete cover coating of 5 mm, in the investigation was used 6 mm to calculate the impact energy for having stricter

conditions. The standard test is for **1** m and the piece weight was calculated by the following equation:

$E_{imp} = m \cdot g \cdot y$ *(Equation 4.1)*,

with E_{imp} = (15 x 6) J = 90 J , g = 9.8 m/s^2 , y = 1 m → m = 9.2 kg (approx.)

Thus, the experimental set-up for the impact test was formed with a wood base to support the pipe and a PVC tube of 160 mm to guide the weight object. The PVC tube was installed on an aluminium frame in such a way that the weight object could vertically fall down and impact on the top central portion of the pile *(Fig. 4.1.a - 4.1.c)*. The weight object with a total mass of 9135 g was formed by a lead (Pb) piece inserted with a hardened steel ball of diameter of 25 mm as an impact point *(Fig. 4.1.b)*.

a)  b) 

c) 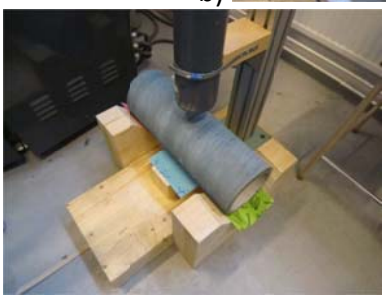

Figure 4.5. a) Developing ZM-U Fabrikstest. b) Weight object for developing ZM-U Fabrikstest. c) Developing ZM-U Fabrikstest.

The weight object was stopped with a nail at the specified level of height before start the impact.

In a first trial the follow specimens were tested:

- Two VRS-ZM specimens - 1 meter (1.A and 1.B).
- Two VRS-ZM specimens - 2 meters (2.A and 2.B).
- Two VRS-ZM specimens - 3 meters (3.A and 3.B).

Furthermore, the following specimens were tested:

- Two VRS-ZM specimens with a radial cut down to the zinc surface (R.A and R.B)

Afterwards, in another trial, the follow specimens were tested:
- Two VRS-PRO specimens - 1 meter (1.AE_p and 1.BE_p).
- Two VRS-PRO specimens - 2 meters (2.AE_p and 2.BE_p).
- One VRS-PRO specimen - 3 meters (3.AE_p).

Moreover, the following specimens were tested:

- Two VRS-ZM specimens (1 and 2 meters – 1.C and 2.C) for have a comparison with the VRS-PRO specimens.
- One VRS-PRO specimen with some sanding of the epoxy layer down to the zinc (R.AE_p).

Finally, to evaluate the damage produced by the test, all the specimens were visually examined after impact steps.

4.2 Salt bath test

After the impact test, the next experiment was prepared. It was started by the VRS-ZM specimens. The goal of this test was accelerate the corrosion process by imposing an external electrical field.

The first thing done for developing this test was to make the lower end of the pipes waterproof, the reason of this decision was to avoid the direct contact between the solution and the ductile iron of the lower end when the pile was immersed in the salt water. Thus, for waterproofing the lower end a plastic disc was glued on the end with silicon and epoxy for preventing the penetration of the solution. In the ductile iron of the upper end a thin hole was drilled for putting a screw, which was used for connecting the cable to the datalogger or power supply. *(Fig. 4.2)*

Figure 4.6. VRS-ZM specimens before put in the salt bath.

Moreover, the salt bath was prepared in plastic boxes with a 5% of NaCl solution. The pipes were immersed to ¾ of their length and each of them was individually connected to the datalogger.

The specimens 1.A, 1.B, 2.A, 2.B, 3.A, 3.B, R.A and R.B were immersed in one salt bath box and two generic specimens of VRS-ZM (G.A and G.B) were immersed in another

box due to the space limitation. A piece of titanium mesh was place in the bottom of each box for electrical connection of the solution.

Thus, the test was started by imposing an external electrical field between the ductile iron (as anode) and the titanium mesh (as cathode) with the purpose to accelerate the corrosion process, but it was proven difficult due to too high current even under a very low potential difference. By this reason it was to try to monitor the open circuit potential of each ductile iron specimen against a gel type of silver-silver chloride (Ag/AgCl) reference electrode, which was connected to the salt bath solution through a salt-bridge with a KCl (3M) solution. The solutions in the two boxes were electrically connected by a plastic tube fully filled with the same salt bath solution. The potential was recorded each 30 minutes by the datalogger. *(Fig. 4.3)*

Figure 4.7. VRS-ZM specimens - salt bath test.

After one month, the monitored results did not give distinguishing information about damage and corrosion. Hence, in the absence of determinant information the salt bath test was used for saturation of the specimens only for the half-cell potential and resistance measurements.

4.2.1 Half-cell potential measurement

After immersion for about one month the VRS-ZM specimens with the salt bath up to ¾ parts of their length were taken out for measuring the half-cell potential with a Calomel reference electrode at different points around the impacted position of the pipe.

Thus, 4 columns (impact column, 10 cm to the left, 10 cm to the right and back column) on each specimen were measured at a spacing of 5 cm in each line. For taking the data a voltmeter was connected to the ductile iron (+) and the Calomel reference electrode (with saturated KCl liquid) (com), whose tip was in contact with a small piece of saturated (5 % NaCl) sponge placed on the measurement point of the pipe surface. Moreover, special attention was paid to the zones with significant difference between the adjacent points, usually in the impact zone.

Furthermore, for preconditioning the VRS-PRO specimens, which were put in a tank with a saturated (5% NaCl) sponge sheet of 20x20 cm covered around the impact zone

and the sponge sheet itself was covered by a plastic sheet to prevent the solution from evaporation *(Fig 4.6 – 4.7)*. The tank was then covered with its cap. In this process the specimens Epoxy 1.AE_p, 1.BE_p, 2.AE_p, 2.BE_p, 3.AE_p, R.AE_p, a generic VRS-PRO specimen G.AE_p and the VRS-ZM specimens 1.C and 2.C were preconditioned. After precondition, the half-cell potential was measured in the same way as describe above, but on three columns (impact column, 5 cm to the left, 5 cm to the right) in 20 cm length covering the impact zone, at a spacing of 2.5 cm in each line. In the zones with significant difference between the adjacent points more data were registered *(Fig 4.4)*.

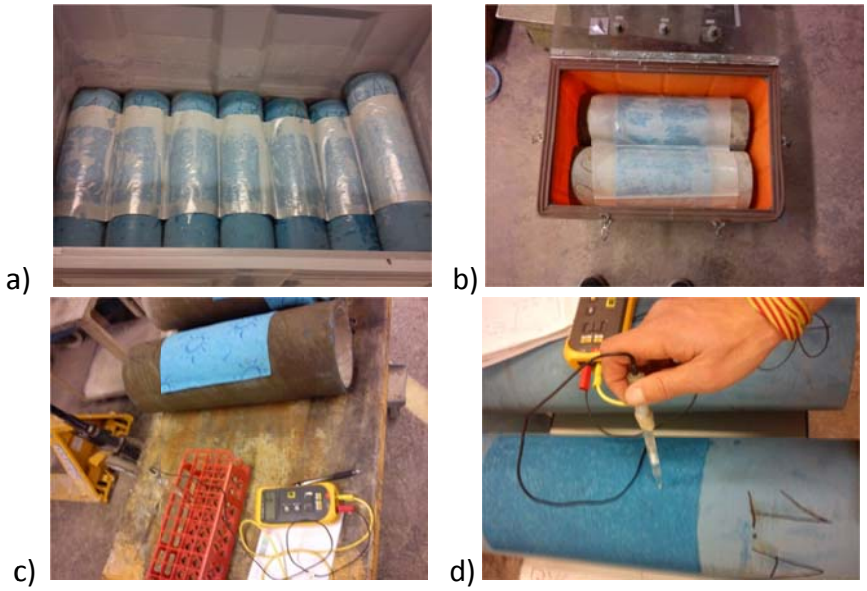

Figure 4.8.a) Preconditioning the VRS-PRO specimens – saturation. b) Preconditioning the VRS-PRO specimens (1.C and 2.C) – saturation. c) Half-cell potential measurement test. d) Half-cell potential measurement test.

4.2.2 Resistance measurement

The next step was to estimate the resistance of the impact zone. The specimens were put in horizontal position and in the impact zone a square (20 cm x 20 cm) sponge layer of 3 mm thickness, saturated with the salt solution (5% NaCl) was placed. A stainless steel mesh was then placed on the sponge layer and a cellulose layer of 50 mm thickness saturated with the same salt solution was placed on the mesh in order to keep the moist condition during the test. The cellulose layer was covered with a steel sheet, on which a weight of 3 kg was placed. *Figure 4.5* illustrates the measurement arrangement.

The stainless steel mesh was connected through an amperemeter to the com-pole of a power supply whose "+" pole was connected to the ductile iron to form a circuit. Thus, after applying supply certain voltage to the circuit both the current (mA) and potential (V) across the stainless steel mesh and the ductile iron were registered. *(Fig 4.5)*

a)  b) 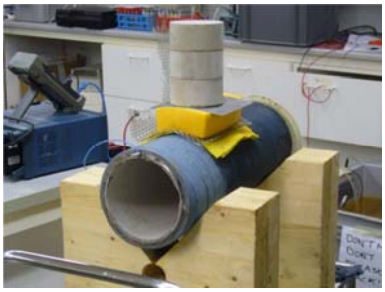

Figure 4.9. Resistance measurement test a) frontal view b) back view.

Firstly, the VRS-ZM specimens were tested. The specimens were saturated with the salt bath, and the data (V' and I) were registered with a power supply of 5 V.

Later, the VRS-PRO specimens, which were preconditioned with saturated sponge in the covered tank as described previously. For these specimens a potential of 1 V was applied due to their relatively low resistance. For some specimens more than one measurement value (V' and I) were registered. Because some specimens had partially unstuck epoxy, the measurements were, therefore, made in the zones with sound epoxy layer as well as with unstuck epoxy.

Finally, the following equation was applied to calculate the resistance of each specimen:

$R_S = 1000 \times V'/ I$ *(Equation 4.2)*

Where R_s has a unit of Ohm while the units of V' and I were V and mA, respectively.

5 ANALYSIS

5.1 Impact test

Once the impact test was applied to the specimen pipes, a visual inspection was carried out in order to evaluate the results.

The test was developed in 3 levels (1, 2 and 3 meters) with the same weight (9.2 kg). Concretely, the energy applied in each level was:

$E_{imp} = m \cdot g \cdot y$ *(Equation 5.1)*,
with $g = 9.8\ m/s^2$, $m = 9.2$ kg (approx)

- y = **1** m

$E_{imp} = 90$ J

- y = **2** m

$E_{imp} = 180$ J

- y = **3** m

$E_{imp} = 270$ J

- First, the VRS-ZM specimens were inspected,

1.A VRS-ZM specimen 1 m (90 J).

After applying the impact test to the 1.A specimen, a thin deformation of 25-30 mm with small cracks was observed on the concrete cover *(Fig. 5.1)*.

a)  b) 

Figure 5.10. 1.A specimen after impact. a) wide external view b) close external view.

1.B VRS-ZM specimen 1 m (90 J).

The 1.B specimen looked similar to the 1.A specimen, with a deformation on the concrete like the dimension of the ball of the weight, and with some small cracks around the impact zone *(Fig. 5.2)*.

a)  b) 

Figure 5.11. 1.B specimen after impact. a) wide external view b) close external view.

1.C VRS-ZM specimen 1 m (90 J).

Just like the previous specimens, the **1**.C presented a small mark on the concrete of the ball of the weight and a circular crack around the pipe *(Fig. 5.3)*.

a)  b) 

Figure 5.12. 1.C specimen after impact. a) wide external view b) close external view.

2.A VRS-ZM specimen 2 m (180 J).

In the 2.A specimen more damage than the previous level specimens was perceived. It presented a hole on the concrete, of 30-35 mm, down to the zinc layer. It was a big crack and in the impact zone the concrete was lightly separated of the zinc layer *(Fig. 5.4)*.

a)  b) 

Figure 5.13. 2.A specimen after impact. a) wide external view b) close external view.

2.B VRS-ZM specimen 2 m (180 J).

The specimen 2.B presented less damage than the 2.A specimen. A little deformation (25-30 mm) on the impact point and some cracks around that point were observed *(Fig. 5.5)*.

a) 

b) 

Figure 5.14. 2.B specimen after impact a) view 1 b) view 2.

2.C VRS-ZM specimen 2 m (180 J).

The result of the impact test in the 2.C specimen was a deformation (30 mm) of the concrete cover in the impact point with cracks around the zone *(Fig. 5.6)*.

a) 
b) 

Figure 5.15. 2.C specimen after impact. a) wide external view b) close external view.

3.A VRS-ZM specimen 3 m (270 J).

This impact level was the most destructive. Thus, the impact test of the 3.A specimen unsticks the concrete cover in the impact zone region. Cracks on the concrete cover around the entire pipe were detected *(Fig. 5.7)*.

a) 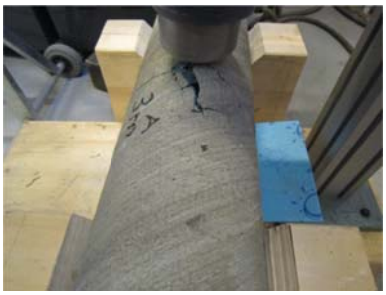
b) 

Figure 5.16. 3.A specimen after impact. a) wide external view b) close external view.

3.B VRS-ZM specimen 3 m (270 J).

In the 3.B specimen the concrete cover was destroyed in the impact point. Moreover, around this point, the concrete cover was unstuck of the zinc layer. Some cracks were detected on the impact region *(Fig. 5.8)*.

a)  b) 

Figure 5.17. 3.B specimen after impact. a) wide external view b) close external view.

R.A and **R.B** VRS-ZM specimens (radial cut).

These specimens looked with a thin line (5 mm) of 10 cm done by a radial machine. The profundity of this crack arrived down to the zinc surface. In radial specimens were not observed another crack on the concrete cover *(Fig. 5.9)*.

a)  b) 

Figure 5.18. R.A and R.B specimens a) Cut test b) wide external view.

-Secondly, the VRS-PRO specimens were observed,

1.AE$_p$ VRS-PRO specimen 1 m (90 J).

In the first VRS-PRO specimen tested, the ball weight was marked in the impact point deforming the iron layer. The epoxy was not unstuck. In the interior were not found cracks in the concrete layer *(Fig. 5.10)*.

a)  b) 

c) 

Figure 5.19. 1.AE$_p$ specimen after impact. a) wide external view b) close external view c) wide internal view.

1.BE$_p$ VRS-PRO specimen 1 m (90 J).

The result appreciated in the 1.BE$_p$ was more or less the same than the 1.AE$_p$, but in the 1.BE$_p$ the deformation had a little bit more profundity. In the interior cracks were not found in the concrete layer *(Fig. 5.11)*.

a)  b) 

c) 

Figure 5.20. 1.BE$_p$ specimen after impact. a) wide external view b) close external view c) wide internal view.

2.AE$_p$ VRS-PRO specimen 2 m (180 J).

In the specimens of 2 meters the deformation in the impact point was more remarkable. The VRS-PRO started to get unstuck of the surface. The inner concrete showed different cracks *(Fig. 5.12)*.

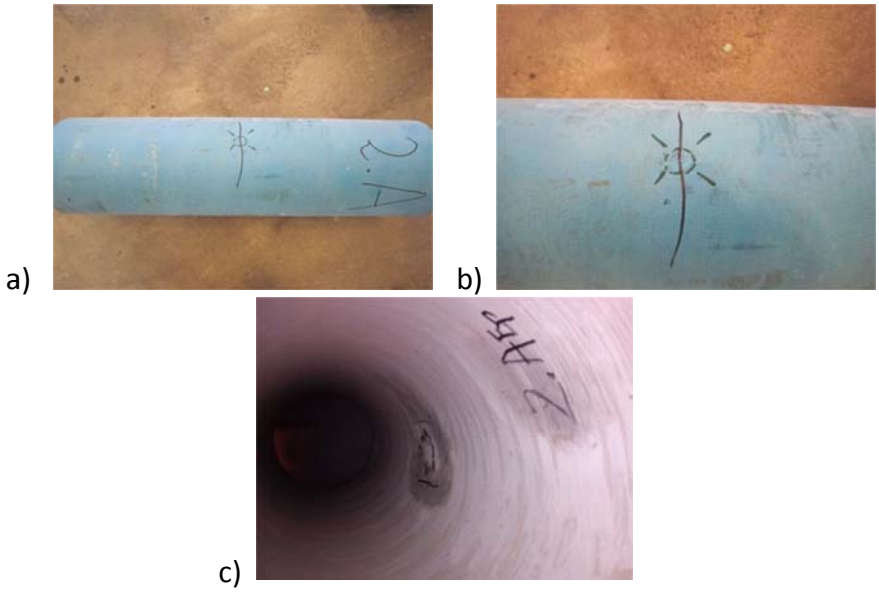

Figure 5.21. 2.AE$_p$ specimen after impact. a) wide external view b) close external view c) wide internal view.

2.BE$_p$ VRS-PRO specimen 2 m (180 J).

This specimen looked similar than the 2.AE$_p$ specimen, but with more deformation in the impact point. Furthermore, the specimen had different points with unstuck epoxy. In the interior, the concrete presented few cracks *(Fig. 5.13)*.

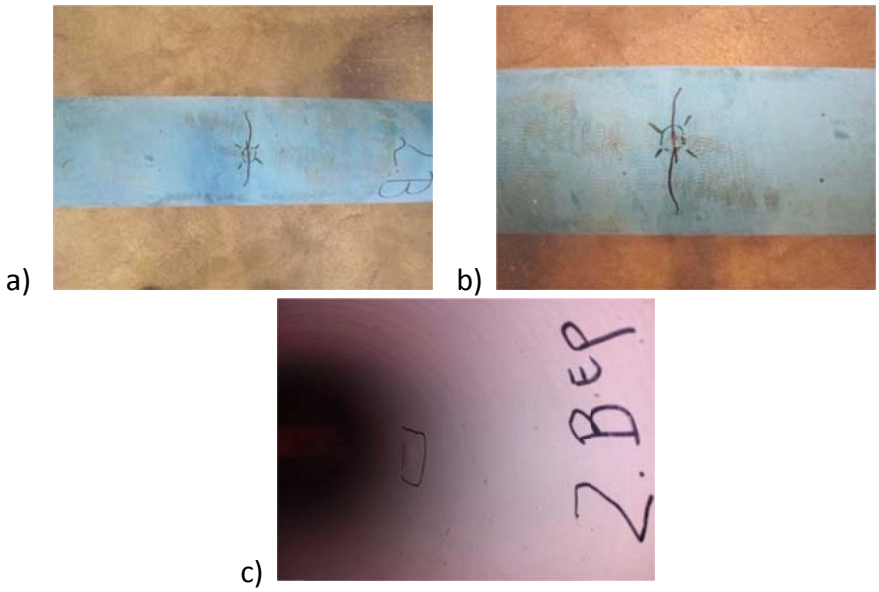

Figure 5.22. 2.BE$_p$ specimen after impact. a) wide external view b) close external view c) wide internal view.

3.AE$_p$ VRS-PRO specimen 3 m (270 J).

This level of impact was the most harmful, causing several damages in the impact zone. The impact marked the ball weight unsticking the epoxy layer and interiorly the concrete coating was practically destroyed *(Fig. 5.14)*.

a)  b) 

Figure 5.23. 3.AE$_p$ specimen after impact. a) wide internal view b) close internal view.

R.AE$_p$ VRS-PRO specimen.

After the sanding of the epoxy layer of R.AE$_p$, the specimen looked perfectly except the sanding region, which had a metal colour, it showed the zinc layer *(Fig. 5.15)*.

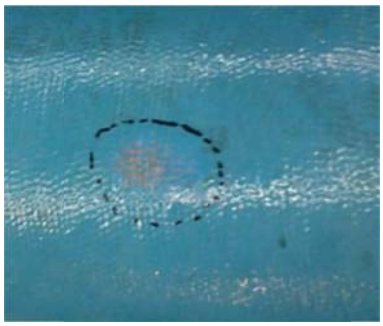

Figure 5.24. Close external view of R.AE$_p$ specimen after sanding.

5.2 Salt bath test

The VRS-ZM specimens were dipped in the salt bath for approximately one month. In this time the measured values were practically constant.

The potential of the ductile iron was recorded every 30 min. Thus, the diagram showed the level of the potential which was, more or less, the same in the first day (from the beginning till the last day) than in the last day. The measured potential values against the gel type of Ag/AgCl reference electrode were in the range of -1500 V and -1770 V for the generic specimens, and between -800 V and -1150 V for the rest of specimens. These negative values imply good protection of iron by the zinc layer. No sudden change of potential was observed, which would be an indication of iron corrosion initiation after failure of zinc protection. Longer exposure period was needed for exhausting the zinc protection layer.

Owing to the limitation of time for an examination work, it was decided to take another way to check the possible corrosion and damage.

5.2.1 Half-cell potential measurement

The half-cell potential at different points on the specimen surface may give us information about the status of zinc protection, which makes the surface potential more negative. To measure the potential map in the VRS-ZM specimens, the data was taken every 5 cm on the right (R), left (L), middle (M) and back (B) of the pipe. In some specimens with significant difference between the center and the sides (R1-L1) other data were measured to evaluate the evolution of the potential. The results obtained in the upper portion of the specimen were not significant at all. These points showed low potentials. The reason why these points showed low potentials was the fact that the specimens were not saturated in this part of the pipe.

G.A – G.B VRS-ZM specimens.

POTENTIAL (V)

G.A	L	M	R	B	G.B	L	M	R	B
20	-190	-270	-450	-260	**20**	-760	-690	-480	-935
15	-680	-600	-580	-430	**15**	-770	-930	-840	-920
10	-872	-850	-850	-815	**10**	-897	-889	-906	-933
5	-950	-949	-902	-960	**5**	-911	-929	-953	-975
0	-953	-964	-953	-953	**0**	-962	-969	-966	-970
-5	-907	-875	-954	-970	**-5**	-966	-968	-974	-983
-10	-902	-895	-898	-915	**-10**	-967	-975	-977	-987
-15	-895	-895	-906	-896	**-15**	-972	-973	-975	-976
-20	-899	-894	-889	-882	**-20**	-960	-964	-973	-980

POTENTIAL DIFFERENCE (V)

G.A	L	M	R	B	G.B	L	M	R	B
5	14	15	62	4	**5**	58	40	16	-6
0	11	0	11	11	**0**	7	0	3	-1
-5	57	89	10	-6	**-5**	3	1	-5	-14

Table 5-4. Potential measurement (V) and potential difference (V) of the specimens G.A and G.B.

The VRS-ZM generic specimens (G.A – G.B) presented ordinary data for a pipe without damage and without high potential difference between closer points. The reason for that low potential from the level +10 was that the pipe was dry from this level. The specimens were saturated with the salt bath up to about 5 cm above the half point.
Hence, the specimens did not have any apparent damage, just a big salt line on the surface *(Fig. 5.16)*.

a)  b) 

Figure 5.25. Half-cell potential measurement a) G.A specimen after saturation b) G.B specimen after saturation.

1.A – 1.B VRS-ZM specimens.

POTENTIAL (V)

1.A		L	M	R	B	1.B		L	M	R	B
	20	-478	-427	-420	-413		**20**	-480	-520	-750	-713
	15	-717	-560	-595	-615		**15**	-640	-680	-806	-730
	10	-846	-835	-830	-744		**10**	-788	-790	-861	-928
	5	-874	-924	-830	-850		**5**	-908	-950	-905	-920
IMPACT	**0**	-870	-940	-852	-846	**IMPACT**	**0**	-936	-960	-913	-933
	-5	-864	-892	-848	-850		**-5**	-910	-950	-910	-915
	-10	-840	-849	-847	-848		**-10**	-917	-915	-910	-908
	-15	-842	-847	-850	-856		**-15**	-913	-915	-907	-908
	-20	-818	-830	-842	-820		**-20**	-908	-907	-902	-888

POTENTIAL DIFFERENCE (V)

1.A		L	M	R	B	1.B		L	M	R	B
	5	66	16	110	90		**5**	52	10	55	40
IMPACT	**0**	70	0	88	94	**IMPACT**	**0**	24	0	47	27
	-5	76	48	92	90		**-5**	50	10	50	45

Table 5-5. Potential measurement (V) and potential difference (V) of the specimens 1.A and 1.B.

The potential measured in the 1.A pipe had not several differences between its selected points, just a positive difference from the impact point. Moreover, the potentials taken about the 1.B specimen did not show any information about damage either, because the difference between the central point and the others were positive and they were not so high.

Furthermore, the results did not give any information about damage and corrosion risk.

As a result, the aspect of the pipes after this test showed just the impact defect *(Fig. 5.17)*.

a)  b) 

Figure 5.26. Half-cell potential measurement a) 1.A specimen after saturation b) 1.B specimen after saturation.

2.A – 2.B VRS-ZM specimens.

POTENTIAL (V)

2.A		**L**	**M**	**R**	**B**	**2.B**		**L**	**M**	**R**	**B**
	20	-890	-838	-810	-916		**20**	-770	-674	-725	-760
	15	-944	-932	-879	-962		**15**	-869	-887	-787	-857
	10	-992	-990	-973	-968		**10**	-951	-965	-930	-885
	5	-1006	-982	-989	-994		**5**	-1001	-1023	-1002	-944
IMPACT	**0**	-1002	-973	-987	-993	**IMPACT**	**0**	-980	-953	-960	-974
	-5	-1001	-993	-991	-988		**-5**	-960	-956	-963	-960
	-10	-996	-998	-993	-997		**-10**	-965	-957	-957	-958
	-15	-995	-991	-988	-990		**-15**	-962	-954	-958	-959
	-20	-985	-997	-985	-979		**-20**	-953	-948	-951	-938

POTENTIAL DIFFERENCE (V)

2.A		**L**	**M**	**R**	**B**	**2.B**		**L**	**M**	**R**	**B**
	5	-33	-9	-16	-21		**5**	-48	-70	-49	9
IMPACT	**0**	-29	0	-14	-20	**IMPACT**	**0**	-27	0	-7	-21
	-5	-28	-20	-18	-15		**-5**	-7	-3	-10	-7

Table 5-6. Potential measurement (V) and potential difference (V) of the specimens 2.A and 2.B.

In the case of two meters specimens, they showed a negative difference between the impact point and the closer points, it could be a possible start of damage, but the difference was too low to conclude anything from it.

The 2.A specimen had less potential difference than the 2.B specimen, which presented a difference of -70 V between the central point and a point 5 cm up. Therefore, it could indicate a possible corrosion risk.

Physically the 2.A pipe suffered a damage of the concrete cover without any hint of damage of the iron-zinc.

Furthermore, the pipe 2.B presented the same aspect of damage than at the beginning of this test, but now it had salt inlaid on the cracks of the concrete cover *(Fig. 18)*.

a)  b) 

Figure 5.27. Half-cell potential measurement a) 2.A specimen after saturation b) 2.B specimen after saturation.

3.A – 3.B VRS-ZM specimens.

POTENTIAL (V)

3.A		**L**	**M**	**R**	**B**	**3.B**		**L**	**M**	**R**	**B**
	20	-806	-820	-925	-805		**20**	-800	-850	-815	-913
	15	(-840,-884)	-940	-954	-930		**15**	-880	-934	-928	-934
	10	-950	-940	-938	-964		**10**	-962	-960	-956	-979
	5	-970	(-890,-840)	-958	-970		**5**	-969	-946	-980	-994
IMPACT	**0**	-967	(-940,-980)	-947	-973	**IMPACT**	**0**	-960	-788	-984	-994
	-5	-967	-970	-984	-980		**-5**	-975	-979	-991	-992
	-10	-989	-994	-991	-970		**-10**	-981	-985	-984	-989
	-15	-987	-992	-995	-965		**-15**	-985	-985	-983	-985
	-20	-972	-974	-972	-950		**-20**	-969	-964	-970	-969

POTENTIAL DIFFERENCE (V)

3.A		**L**	**M**	**R**	**B**	**3.B**		**L**	**M**	**R**	**B**
	5	-30	100	-18	-30		**5**	-181	-158	-192	-206
IMPACT	**0**	-27	0	-7	-33	**IMPACT**	**0**	-172	0	-196	-206
	-5	-27	-30	-44	-40		**-5**	-187	-191	-203	-204

Table 5-7. Potential measurement (V) and potential difference (V) of the specimens 3.A and 3.B.

After carrying out the study of the data of the 3.A specimen, a possible damage was observed. The data showed a lower potential point in the center 5 cm up of the impact point, because of that it was decided to measure the potential in this region again.

POTENTIAL' 3.A (V)

3.A		**L**	**M**	**R**		**L-M**	**M**	**M-R**
	15				**5**	-767	-850	-885
	10					-934	-949	-896

	5	-973	-965	-969		-965		-934
IMPACT	**0**	-975	-948	-970	**0**	-961	-949	-936
	-5	-980	(-965,-945)	-975				
	-10							
	-15				**-5**		-950	

POTENTIAL DIFFERENCE' 3.A (V)

3.A		**L**	**L-M**	**M**	**M-R**	**R**
	5	-206	0	-83	-118	-202
			-167	-182	-129	
			-198		-167	
IMPACT	**0**	-208	-194	-182	-169	-203
	-5	-213		-183		-208

Table 5-8. Potential' measurement (V) and potential difference' (V) of the specimens 3.A.

The new results were taken depending on the difference between the points. First, it was the current points, and afterwards more points were exhaustively taken, namely between -5 to 5 from the left to the right.
The data were measured directly on the zinc layer with a small piece of sponge, after moving off the damaged concrete cover, which was unstuck.

Thus, the point with less negative potential was 5 cm up and to the left of the impact point. This point showed high differences with the closer points. Possible reason might be that in this unstuck area the zinc layer was not homogeneous and the point with less negative potential hade thinner zinc layer which was exhausted and lost its protection function.

The specimen 3.B presented a high potential difference between the impact point and the closer points after moving off the concrete cover unstuck and measuring the potential on the zinc layer with a small piece of sponge,. As a result, it was possible to conclude the start of damage in the central point.

Furthermore, these specimens presented an aspect with different points and regions with white and brown marks *(Fig. 5.19)*.

a)  b) 

c)

d)

e)

Figure 5.28. Half-cell potential measurement a) 3.A specimen after saturation b) 3.A specimen after saturation with the concrete cover unstuck – wide external view c) 3.A specimen after saturation with the concrete cover unstuck – close external view d) 3.B specimen after saturation b) 3.B specimen after saturation with the concrete cover unstuck – close external view.

R.A – R.B VRS-ZM specimens.

POTENTIAL (V)

R.A		L1	L	M	R	R1	B	R.B		L1	L	M	R	R1	B
	20		-338	-338	-391		-297		**20**		-354	-365	-362		-390
	15		-430	-519	-558		-438		**15**		-447	-460	-446		-507
	10		-554	-687	-710		-557		**10**		-593	-560	-525		-615
	5		-667	-698	-727		-606		**5**		-730	-724	-712		-802
CUT	**0**	-712	-584	-520	-490	-720	-969	**CUT**	**0**	-751	-775	-764	-770	-754	-751
	-5		-718	-715	-724		-740		**-5**		-765	-762	-748		-751
	-10		-723	-727	-748		-722		**-10**		-758	-756	-752		-810
	-15		-725	-740	-729		-720		**-15**		-777	-791	-770		-753
	-20		-701	-708	-722		-710		**-20**		-767	-757	-755		-751

POTENTIAL DIFFERENCE (V)

R.A		L1	L	M	R	R1	B	R.B		L1	L	M	R	R1	B
	5		-177	-208	-237		-116		**5**		34	40	52		-38
CUT	**0**	-222	-94	-30	0	-230	-479	**CUT**	**0**	13	-11	0	-6	10	13
	-5		-228	-225	-234		-250		**-5**		-1	2	16		13

Table 5-9 Potential measurement (V) and potential difference (V) of the specimens R.A and R.B.

In the R.A pipe it could be observed the possible damage from the central point and between the center and the right part. It showed the evolution of the potential difference in a short space.

The result of this test in R.B specimen did not reveal any significant information. After comparing these results to the R.A specimen it was thought that there should be some abnormal data, because of the high different results.
Thus, the 3.B specimen was measured again, and the results were the same. The reason of this result may be a less profundity of the radial cut.

Moreover, the aspect of the specimens showed a viscous and white-yellow coloured substance on the cut *(Fig. 5.20)*.

a) 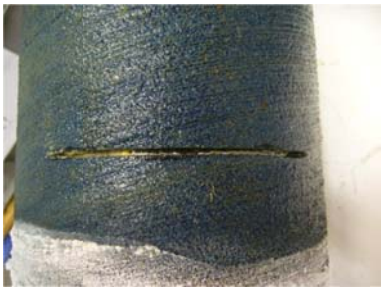 b) 

Figure 5.29. Half-cell potential measurement a) R.A specimen after saturation b) R.B specimen after saturation.

Thus, once finished the trial for the VRS-ZM specimens, the half-cell potential was measured on the remaining specimens.

Another way was taken to measure the half-cell potential, because these pipes were differently saturated. More data were taken in the central zone. They were registered on three columns (impact column, 5 cm to the left, 5 cm to the right and some specimens in the middle of these columns) in 20 cm length covering the impact zone, at a spacing of 2.5 cm on each line. In the zones with significant differences between the adjacent points, more data were registered.

1.C VRS-ZM specimen.

POTENTIAL (V)

1.C		**L1**	**L**	**M**	**R**	**R1**
	10	-957		-946		-943
	7.5	-953		-945		-944
	5	-951		-944		-945
	2.5	-950		-940		-945
IMPACT	**0**	-958	-941	-934	-944	-945
	-2.5	-950		-938		-942
	-5	-948		-946		-944
	-7.5	-949		-950		-949
	-10	-949		-954		-949

POTENTIAL DIFFERENCE (V)

1.C		L1	L	M	R	R1
	7.5	-19		-11		-10
	5	-17		-10		-11
	2.5	-16		-6		-11
IMPACT	**0**	-24	-7	0	-10	-11
	-2.5	-16		-4		-8
	-5	-14		-12		-10
	-7.5	-15		-16		-15

Table 5-10. Potential measurement (V) and potential difference (V) of the specimen 1.C.

The results of the tests did not reveal any information about a possible damage or corrosion sign, like the 1.A and 1.B specimens. Thus, the image presented by this specimen after the tests was just the damage caused by the impact test.

2.C VRS-ZM specimen.

POTENTIAL (V)

2.C		L1	L	M	R	R1
	10	-911		-912		-908
	7.5	-913		-910		-912
	5	-909		-906		-911
	2.5	-910		-906		-910
IMPACT	**0**	-915	-900	-905	-907	-910
	-2.5	-918		-908		-911
	-5	-919		-909		-907
	-7.5	-922		-916		-911
	-10	-923		-921		-913

POTENTIAL DIFFERENCE (V)

2.C		L1	L	M	R	R1
	7.5	-8		-5		-7
	5	-4		-1		-6
	2.5	-5		-1		-5
IMPACT	**0**	-10	5	0	-2	-5
	-2.5	-13		-3		-6
	-5	-14		-4		-2
	-7.5	-17		-11		-6

Table 5-11. Potential measurement (V) and potential difference (V) of the specimen 2.C.

This specimen did not show high potential difference between the points measured. Thus, it could be concluded that the 2.C pipe did not have any damage on the zinc-iron surface.

Consequently, the defect observed was the damage produced by the impact test.

G.AE$_p$ VRS-PRO specimen.

POTENTIAL (V)

G.AEp		L1	M	R1
	10	-983	-983	-981
	7.5	-985	-984	-982
	5	-986	-985	-981
	2.5	-988	-986	-981
	0	-989	-985	-984
	-2.5	-989	-986	-984
	-5	-988	-986	-984
	-7.5	-989	-987	-983
	-10	-991	-987	-983

POTENTIAL DIFFERENCE (V)

G.AEp		L1	M	R1
	7.5	-0	1	3
	5	-1	0	4
	2.5	-3	-1	4
	0	-4	0	1
	-2.5	-4	-1	1
	-5	-3	-1	1
	-7.5	-4	-2	2

Table 5-12. Potential measurement (V) and potential difference (V) of the specimen G.AE$_p$.

According to the potentials values determined, it was concluded that the generic specimen had ordinary potentials; just as a specimen with no damage.
Therefore, the final image was a specimen as an ordinary pipe.

1.AE$_p$ – 1.BE$_p$ VRS-PRO specimens.

POTENTIAL (V)

1.AEp		L1	M	R1	1.BEp		L1	M	R1
	10	-988	-989	-990		**10**	-1012	-1012	-1008
	7.5	-990	-990	-991		**7.5**	-1011	-1010	-1008
	5	-991	-991	-991		**5**	-1008	-1008	-1007
	2.5	-991	-991	-991		**2.5**	-1007	-1007	-1005
IMPACT	**0**	-991	-982	-991	**IMPACT**	**0**	-1005	-1001	-1005
	-2.5	-989	-988	-990		**-2.5**	-1004	-1003	-1002
	-5	-991	-990	-990		**-5**	-1003	-1002	-1001
	-7.5	-998	-993	-991		**-7.5**	-1002	-1002	-1001
	-10	-998	-992	-991		**-10**	-1002	-1001	-1002

POTENTIAL DIFFERENCE (V)

1.AE$_p$		**L1**	**M**	**R1**	**1.BE$_p$**		**L1**	**M**	**R1**
	7.5	-8	-8	-9		**7.5**	-5	-5	-1
	5	-9	-9	-9		**5**	-4	-3	-1
	2.5	-9	-9	-9		**2.5**	-1	-1	0
IMPACT	**0**	-9	0	-9	**IMPACT**	**0**	0	0	2
	-2.5	-7	-6	-8		**-2.5**	2	6	2
	-5	-9	-8	-8		**-5**	3	4	5
	-7.5	-16	-11	-9		**-7.5**	4	5	6

Table 5-13. Potential measurement (V) and potential difference (V) of the specimens 1.AE$_p$ and 1.BE$_p$.

The potentials values observed in these specimens showed a close relation between themselves. Hence, the specimens presented low potential difference between all the measured points. Thus, it could not be concluded the presence of damage or corrosion.

From that moment on, the specimens did not have more visible damage but the one produced by the impact.

2.AE$_p$ – 2.AE$_p$ VRS-PRO specimens.

POTENTIAL (V)

2.AEp		**L1**	**L**	**M**	**R**	**R1**	**2.BEp**		**L1**	**L**	**M**	**R**	**R1**
	10	-989		-986		-986		**10**	-981		-977		-976
	7.5	-987		-985		-984		**7.5**	-980		-974		-977
	5	-987		-980		-982		**5**	-983		-967		-970
	2.5	-988		-975		-981		**2.5**	-972		-942		-965
IMPACT	**0**	-989	-970	-943	-976	-982	**IMPACT**	**0**	-966	-950	-835	-947	-968
	-2.5	-988		-974		-987		**-2.5**	-954		-930		-957
	-5	-987		-980		-986		**-5**	-963		-943		-958
	-7.5	-988		-986		-988		**-7.5**	-967		-962		-965
	-10	-991		-989		-991		**-10**	-973		-974		-968

POTENTIAL DIFFERENCE (V)

2.AEp		**L1**	**L**	**M**	**R**	**R1**	**2.BEp**		**L1**	**L**	**M**	**R**	**R1**
	7.5	-44		-42		-41		**7.5**	-145		-139		-142
	5	-44		-37		-39		**5**	-148		-132		-135
	2.5	-45		-32		-38		**2.5**	-137		-107		-130
IMPACT	**0**	-46	-27	0	-33	-39	**IMPACT**	**0**	-131	-115	0	-112	-133
	-2.5	-45		-31		-44		**-2.5**	-119		-95		-122
	-5	-44		-37		-43		**-5**	-128		-108		-123
	-7.5	-45		-43		-45		**-7.5**	-132		-127		-130

Table 5-14. Potential measurement (V) and potential difference (V) of the specimens 2.AE$_p$ and 2.AE$_p$.

Pursuant to the potentials obtained in the 2.AE_p it could observed a small potential difference between the central point and the others. Consequently, it could be a sign of the beginning of the corrosion.

However, the values measured in the 2.BE_p specimen showed a high potential difference between the impact point and the rest of points. Thus, this difference could indicate damage in the iron-zinc surface.

Moreover, the final appearance of the specimens was a mark with the epoxy layer unstuck in the impact zone *(Fig. 5.21)*.

a)  b) 

Figure 5.30. Half-cell potential measurement a) 2.AE_p specimen after saturation b) 2.BE_p specimen after saturation.

3.AE_p VRS-PRO specimen.

POTENTIAL (V)

3.AEp		**L2**	**L1**	**L**	**M**	**R**	**R1**	**R2**
	10	-983			-988			-988
	7.5	-983			-984			-985
	5	-979			-981			-985
	2.5	-976			-973			-980
IMPACT	**0**	-970	-949	-914	-805	-920	-941	-971
	-2.5	-964			-920			-963
	-5	-963			-939			-962
	-7.5	-973			-980			-975
	-10	-979			-980			-983

POTENTIAL DIFFERENCE (V)

3.AEp		**L2**	**L1**	**L**	**M**	**R**	**R1**	**R2**
	7.5	-178			-179			-180
	5	-174			-176			-180
	2.5	-171			-168			-175
IMPACT	**0**	-165	-144	-109	0	-115	-136	-166
	-2.5	-159			-115			-158
	-5	-158			-134			-157
	-7.5	-168			-175			-170

Table 5-15. Potential measurement (V) and potential difference (V) of the specimen 3.AE$_p$.

According to the potentials obtained in the 3 meters VRS-PRO specimen, it could be observed a several potential difference in the impact zone. Hence, the damage of iron-zinc layer could be localized in this region.

Furthermore, the specimen had an aspect of the mark of approximately 3x6 cm with the epoxy layer unstuck *(Fig. 5.22)*.

Figure 5.31. Half-cell potential measurement - 3.AE$_p$ specimen after saturation.

R.AE$_p$ VRS-PRO specimen.

POTENTIAL (V)

R.AEp		L1	L	M	R	R1
	10	-1010		-1010		-1009
	7,5	-1010		-1009		-1009
	5	-1008		-1009		-1009
	2.5	-1008		-1009		-1008
SANDING	**0**	-1007	-1008	-1023	-1008	-1007
	-2.5	-1007		-1008		-1007
	-5	-1006		-1007		-1006
	-7.5	-1004		-1003		-1005
	-10	-1001		-1001		-1003

POTENTIAL DIFFERENCE (V)

R.AEp		L1	L	M	R	R1
	7.5	13		14		14
	5	15		14		14
	2.5	15		14		15
SANDING	**0**	16	15	0	15	16
	-2.5	16		15		16
	-5	17		16		17
	-7.5	19		20		18

Table 5-16 Potential measurement (V) and potential difference (V) of the specimen R.AE$_p$.

Finally, the sanded VRS-PRO specimen presented the typical potentials of a specimen without any damage, the potential difference between its points was really low. Thus, there was not any presence of a possible damage on the iron-zinc layer.
The final image of this specimen had a silver mark representing the zinc surface of approximately 2x4 cm, with some blue points of epoxy *(Fig. 5.23)*.

Figure 5.32. Half-cell potential measurement - R.AE$_p$ specimen after saturation.

5.2.2 Resistance measurement

The last test done was to estimate the resistance of the specimens in the impact zone, which may give us information about the degree of damage in the cover layer. In the test the values of V_0 (power supply - V), I (current in the circuit - mA), and V' (voltage across the electrode and the iron - V) were measured and the values of R_s (resistance of the specimen - Ohm) and R_A (amperemeter resistivity - Ohm) were calculated by the following equations:

$R_s = 1000 \times V'/I$ *(Equation 5.2)*
$R_A = 1000 \times (V_0 - V')/I$ *(Equation 5.3)*

$R_s + R_A = 1000V_0/I - R_A$ *(Equation 5.4)*

Firstly, the values of VRS-ZM specimens were taken. The results were registered when the **V'** and **I** were constant. Thus, the generic specimens were measured in different points of the pipe center, the rest of specimens were tested just in the impact zone.

G.A – G.B VRS-ZM specimen.

G.A	**V_0**	**I**	**V'**	**R_S**	**G.B**	**V_0**	**I**	**V'**	**R_S**
	5	30.1	4.83	160.3		5	28.1	4.84	172.2
	5	33.3	4.81	144.4		5	32.6	4.81	147.6
	5	42.2	4.76	112.7		5	26.8	4.85	180.8
	5	29.3	4.83	164.9					

Table 5-17. Resistance measurement of the specimens G.A and G.B.

Hence, the **generic** specimens had a concordance between themselves, with an average of **R_s = 161.7** Ohm, with an exception of the third G.A value (R_s = 112.7). In this

position a crack on the concrete cover was observed, it could be the reason of this low result for a generic specimen.

From the measurement of these specimens, the average value of the resistance of the amperemeter used was R_A = 5.78 Ohm

1.A – 1.B – 1.C VRS-ZM specimen.

1.A	**V_0**	**I**	**V'**	**R_S**	**1.B**	**V_0**	**I**	**V'**	**R_S**	**1.C**	**V_0**	**I**	**V'**	**R_S**
	5	28.7	4.83	168.4		5	31.3	4.82	154		5	37.2	4.78	128.5

Table 5-18. Resistance measurement of the specimens 1.A, 1.B and 1.C.

The results of **one** meter specimens were really similar to the generic specimens, with an average of **R_s = 150.3** Ohm. Thus, it showed the low damage of this type of pipes.

2.A – 2.B – 2.C VRS-ZM specimen.

2.A	**V_0**	**I**	**V'**	**R_S**	**2.B**	**V_0**	**I**	**V'**	**R_S**	**2.C**	**V_0**	**I**	**V'**	**R_S**
	5	74.5	4.57	61.3		5	58	4.66	80.4		5	68.5	4.6	67.2

Table 5-19. Resistance measurement of the specimens 2.A, 2.B and 2.C.

According to the values of the **two** meters specimens it could observe an indication of a possible damage. Thus, the 2.A (R_s = 61.3) was the specimen with less resistance, which is an indication of a higher conductivity and corrosion risk. The average of **R_s = 69.6** Ohm is less than the average of the generic specimens.

3.A – 3.B VRS-ZM specimen.

3.A	**V_0**	**I**	**V'**	**R_S**	**3.B**	**V_0**	**I**	**V'**	**R_S**
	5	141.7	4.2	29.5		5	240	3.61	15.1

Table 5-20. Resistance measurement of the specimens 3.A and 3.B.

The resistance values calculated in the **three** meters specimen showed a clear evidence of damage. Anyway, the 3.B (R_s = 15.1) specimen had lower resistance than the 3.A (R_s = 29.5) specimen, with a consequence of a high corrosion risk.

R.A – R.B VRS-ZM specimen.

R.A	**V_0**	**I**	**V'**	**R_S**	**R.B**	**V_0**	**I**	**V'**	**R_S**
	5	145	4.2	28.7		5	92.6	4.47	48.2

Table 5-21. Resistance measurement of the specimens R.A and R.B.

Pursuant to the resistance obtained in the **radial cut** specimens, a clear difference between themselves was observed. The R.A (R_s = 28.7) specimen had approximately

the half of resistivity than the R.B (R_s = 48.2), with similar value to the 3.A (R_s = 29.5) specimen. Furthermore, it could be concluded the level of damage in these specimens would be between the 2 and 3 meters specimens.

Finally, the tests consisted of measuring the values to calculate the resistance of the VRS-PRO specimens. Thus, the generic specimen was calculated in two points, and the 2 and 3 meters specimens were measured with the epoxy layer and without this layer unstuck (No Epx).

G.AE$_p$ VRS-PRO specimen.

G.AEp	**V_0**	**I**	**V'**	**R_S**
	1	35	0.8	22.8
	1	32	0.82	25.5

Table 5-22. Resistance measurement of the specimen G.AEp.

Once the **generic** specimen was observed, it showed an average of **R_s = 24.1** Ohm, which was a reference without any type of damage.

1.AE$_p$ – 1.BE$_p$ VRS-PRO specimen.

1.AEp	**V_0**	**I**	**V'**	**R_S**	**1.BEp**	**V_0**	**I**	**V'**	**R_S**
	1	41	0.77	18.7		1	34	0.81	23.7

Table 5-23. Resistance measurement of the specimens 1.AE$_p$ and 1.BE$_p$.

Thus, the **one** meter specimens revealed results similar to the generic specimen, it could lead to the deduction of an absence or partial absence of damage. Moreover, the specimen 1.AE$_p$ would have more possibility to have corrosion problems, due to its slightly low resistance.

2.AE$_p$ – 2.BE$_P$ VRS-PRO specimen.

2.AEp	**V_0**	**I**	**V'**	**R_S**	**2.BEp**	**V_0**	**I**	**V'**	**R_S**
	1	51	0.71	13.8		1	35	0.8	22.8
	1 (No Epx)	81.5	0.53	6.5		1 (No Epx)	77.5	0.56	7.2

Table 5-24. Resistance measurement of the specimens 2.AE$_p$ and 2.BE$_p$.

According to the resistance calculated in the **two** meters specimens, several conclusions could be stated. First, the specimen with the epoxy layer would be more protected under corrosion, as it had a relatively higher resistance. The 2.AE$_p$ (R_s = 13.8 Ohm) had less resistance than the 2.BE$_p$ (R_s = 22.8 Ohm), anyway this last value is really similar to the generic and one meter specimens.

Furthermore, when the epoxy layer unstuck was moved off, the resistance value was really low, with an average of **R_s = 6.84** Ohm. This result could be an indication of high corrosion risk.

3.AE_p VRS-PRO specimen.

3.AEp	**V_0**	**I**	**V'**	**R_S**
	1	51.2	0.71	13.8
	1 (No Epx)	66	0.62	9.39

Table 5-25. Resistance measurement of the specimen 3.AE_p.

The resistance values obtained in the **three** meters specimen had results similar to the two meters specimen. Consequently, the resistance measured with the epoxy layer was really close to the 2.AE_p specimen. Moreover, the value without the epoxy layer was low, but it was relatively high comparing to the two meters specimens, probably due to different unstuck areas.

R.AE_p VRS-PRO specimen.

R.Aep	**V_0**	**I**	**V'**	**R_S**
	1	83	0.52	6.27

Table 5-26. Resistance measurement of the specimen R.AE_p.

The last specimen tested was the **sanding** specimen, which showed different results from the other specimens. It was the specimen with less resistance calculated. This low resistance is expected because of the loss of the electrically resistant epoxy layer. As indicated from the results of half-cell potential measurement, there is no significant potential difference on the sanding area, implying that if no damage on the zinc layer, this low resistance will not indicate a risk of corrosion.

5.3 Summary

According to the study developed previously, a global analysis was carried out by the impact levels.

The general behaviour observed in the **one meter** specimens was a good structural condition after impacting. Anyway, the results obtained in the “half-cell potential measurement” and “resistance measurement” could lead to the deduction of an absence or partial absence of damage and corrosion risk.

Moreover, for this conditions both the VRS-ZM specimens and the VRS-PRO specimens had a good protection from impact (one meter) and from corrosion. Consequently, they should have a similar service life.

Pursuant to the structural examination done in the **two meters** specimens, the VRS-ZM specimens only had some cracks on the external concrete cover. However, the VRS-PRO specimens showed good external conditions, but the internal concrete coating had several cracks, which could affect the structural life of the pipe.

Furthermore, the VRS-ZM specimens showed that the concrete cover is a good protection in the short-term from corrosion risk, but in the long term the corrosion could start to appear. Anyway, the analysis done in the VRS-PRO specimens could indicate a beginning of corrosion, but in the unstuck epoxy zones (due to the impact) the specimens had a high corrosion risk and damage.

After studying the structural results observed in the **three meters** specimens it was possible to observe a high external damage when taking off the concrete cover in the case of VRS-ZM specimens and the epoxy layer in the other ones. Moreover, the VRS-PRO specimen showed a high damage in the internal concrete coating.

Furthermore, the specimens showed high corrosion risk in the impact zone. Hence, when the concrete cover or the epoxy layer, depending on the type of specimen, was highly damaged the corrosion risk was higher.

The **radial cut** (VRS-ZM) specimens showed a clear damage and corrosion risk in the zone with absence of concrete (cut zone), where the zinc layer was in contact with the exterior.

The structural behaviour would be the normal, because the specimens only have a punctual cut in the concrete.

Regarding the aspect showed by the **sanding** (VRS-PRO) specimen it could be concluded that the specimen had good structural conditions after the trials. Besides, the specimen did not present any indication of damage in the “half-cell potential measurement” test, although in the “resistance measurement” the resistance was very low, due to the loss of high resistant epoxy layer. If there is no damage on the zinc layer, it should, however, have no risk of corrosion after sanding.

Moreover, the VRS-ZM specimens have better structural conditions.

Finally, the next tables show a summary of the damage and corrosion risk among other factors against the different impact energies. Firstly for the VRS-ZM pipe, later for the VRS-PRO pipe and a comparison table between both pipes at the end.

Sample	Impact energy	External damage	Intenal damage	Concrete damage	Potential difference	Resistance (Ohm)
G.A	-	-	-	-	-	140
G.B	-	-	-	-	-	160
1.A	90 J	+	-	-	-	168
1.B	90 J	+	-	-	-	154
1.C	90 J	+	-	-	-	128
2.A	180 J	++	-	+	+	61
2.B	180 J	++	-	+	+	80
2.C	180 J	+	-	-	-	62
3.A	270 J	+++	-	++	+++	29.5
3.B	270 J	+++	-	++	+++	15.1
R.A	CUT	+	-	-+	++	28.7
R.B	CUT	+	-	-+	-	48.7

Table 5-274. Summary VRS-ZM specimens.

Sample	Impact energy	External damage	Intenal damage	Epoxy damage	Potential difference	Resistance (Ohm)
G.AEp	-	-	-	-	-	23
G.BEp	-	-	-	-	-	25
1.AEp	90 J	-	-	-	-	19
1.BEp	90 J	-	-	-	-	24
2.AEp	180 J	+	+	++	+	14/6.5
2.BEp	180 J	+	-+	++	+	22.8/7.2
3.AEp	270 J	++	+++	++	+++	13.8/7.2
R.AEp	SANDING	+	-	+	-	6.27

Table 5-285. Summary VRS-PRO specimens.

VRS-ZM	Concrete protection	Possible Zinc damage	Corrosion risk	Internal Failure
90 J	√ √	√ √	√ √	√ √
180 J	√	x	x	√ √
270 J	√ / x	xx	xxx	√ √
Cut	x	xx	xx	√ √

VRS-PRO	Epoxy protection	Possible Zinc damage	Corrosion risk	Internal Failure
90 J	√ √	√ √	√ √	√
180 J	√ / x	x	x	x
270 J	x	xx	xxx	xx
Sanding	x	x	x	√ √

√ Good quality x Bad quality

Table 5-296. Comparison VRS-ZM - VRS-PRO

6 CONCLUDING REMARKS AND SUGGESTIONS

This study started with a literature review of the research topic studied, with special attention to the zinc properties and a remark of the soil classification depending on its level of corrosion. The study of the structural behaviour of the cover layer was focused on the impact test ZM-U Fabrikstest (7.2.3 SS-EN 15542:2008). Two short term laboratory tests, a Half-cell potential measurement and a resistance measurement were developed in order to estimate the corrosion risk and the possible damage of both types of pipes.

The study of the literature revealed that several factors have an influence on the thickness and formation of the zinc coating (the bath temperature, the dipping time, the cooling rate, and the steel properties, especially the content of silicon in the steel) and the formation of the passive layer of the hot-dip galvanised steel (the composition of the chromate solution used, its pH value, the temperature, the quality of the coating, and the state of the surface), which are linked to the durability and service life of hot-dip galvanised steel. Moreover, the study showed the importance of an exterior cover layer for protecting the ductile iron under corrosion.

Thus, after applying the impact test ZM-U Fabrikstest, it was concluded that both kinds of pipes had good structural conditions under impacts of energy of 90 J. For this level of impact the structural performance of the concrete cover and the epoxy cover layer could undergo a normal service life.

Furthermore, a VRS-ZM pipe would have the initial structural conditions after applying an energy impact of 180 J, but with some exterior cracks; a VRS-PRO pipe would start to have some problems in the structural life of the pipe after an impact energy of 180 J, as it suffered several interior cracks.

However, for an impact energy of 270 J both kinds of pipes would impair structural life conditions, specially the Epoxy layer pipe.

According to the laboratory tests it can be concluded that, under an impact energy of 90 J and 180 J, VRS-ZM pipe revealed relatively good performance of the concrete cover for protecting the pipe from damage of the iron-zinc layer.

Nevertheless VRS-PRO pipe, with an impact energy of 180 J, would have a high corrosion risk and possible damage on the impact zone with the epoxy layer unstuck; while for an impact energy of 90 J it would have good performance.

Besides, an impact energy of 270 J both kinds of specimens showed a high corrosion risk and possible damage, which may shorten the service life of the pipes. Furthermore, VRS-ZM pipes with a crack/cut on the concrete cover of 10 cm x 5 mm down to the zinc layer would have several possibilities of damage and corrosion risk; nonetheless a sanding epoxy layer for the other specimen would not have problems of damage and corrosion risk.

Thereby, the concrete cover for protection of ductile iron pipes (VRS-ZM) has a good performance under impacts (between 0 J and 180 J) that may happen during the installation phase. Moreover, for high impacts >180 J and for specimens with big cut/crack, it would be recommendable to control and repair the cut area to prevent possible corrosion or damage on the iron-zinc layer. Nevertheless for very high impacts >270 J the performance of the concrete cover would be become very poor if no repair action is taken, thus it is recommendable to repair the zone according to the catalogue "Gustavsberg Rörsystem. *VRS SYSTEM - Ett komplett system rör och rördelar med dragsäkra fogar*", or simply to replace the damaged pipe.

The epoxy layer cover for protection of ductile iron pipe (VRS-PRO) has a good performance under impacts around 90 J. For higher impacts they may have corrosion risk and possible damage of the internal concrete, which would be impair its service life in the long-term. Moreover, for this kind of pipe, a specimen with an absence of epoxy layer (sanding test) in some zones, it would be recommendable to control and repair the sanded area to prevent possible corrosion or damage on the iron-zinc layer.

According to the conclusions taken from Korrosioninstutet (KIMAB) studies (Chapter 3.1 - "Swedish soil properties") the ductile iron pipes may have good behaviour against corrosion in Göteborg soils and normal service life when the zinc covers throughout the ductile-iron surface. However, when the zinc layer starts to inhibit, the corrosion risk is high in Göteborg soils. Thus, it would be recommendable to control this possible damage during the service life of the pipe.

Moreover, for the studied pipes, under Göteborg soil conditions, pitting corrosion could occur due to the chloride ions presence in Göteborg (close to the sea) and the possible damaged zinc in both specimens after impact energies > 180 J and with several cracks (sanding) on the surface.

In brief, the concrete cover for ductile iron pipes (VRS-ZM) would have better performance than the epoxy coating layer for ductile iron pipes (VRS-PRO) under the same conditions. However, the VRS-PRO pipe has the advantage of less dimension than the VRS-ZM pipe. Thus, if no space limitation in the installation site, it would be recommendable to use the VRS-ZM type of pipe.

Furthermore, since the end of 2010 a new Standard (SS - EN 545:2010) was introduced for the concrete cover on the ductile iron pipe for water supplying. According to this Standard the thickness of ductile iron can be reduced as half as previous one (e.g. from previous 6 mm to 3 mm). This puts high requirements on the quality of concrete cover in order not to be damaged under the installation phase, in which possible shock impact may happen. The cover is made of a thin layer of fibre reinforced concrete with a layer of epoxy resin between the concrete and the iron pipe. Up to now there is a lack of information about the effect of impacts under installation on the performance of concrete cover of this new type of pipe. To ensure the service life of the pipe for water supplying, there is a need to evaluate this effect.

Due to the lack of model and standard test methods for service life of ductile iron pipe, this study was limited to the laboratory test as a pilot trial for estimation of corrosion risk of the pipe subjected to impacts. Further research work is needed to test the corrosion under the Göteborg soil parameters (in the installation area) and evaluate the possible consequences that would happen on the ductile iron pipes during their service life.

7 REFERENCES

Aal, E.E. Abd El, and S. Abd El Wanees (2009). *Galvanostatic study of the breakdown of Zn passivity by sulphate anions*. Corrosion Science, pp. 1780-1788.

Alonso, C., Sánchez, J., Fullea, J., Andrade, C., Tierra, P., Bernal, M. (2000). *The Addition of Ni to Improve the Corrosion Resistance of Galvanized Reinforcement.* 19th Intern. Galvanizing Conference and Exhibition. Intergalva, Berlin, Germany.

American Water Works Association (AWWA), (2009). *Ductile-Iron Pipe and Fittings - Manual of Water Supply Practices, M41. (3rd Edition)*.

American Water Works Association. *Standard for Polyethylene Encasement for Ductile-Iron Pipe Systems. ANSI/ AWWA C105/A21.5.* Denver, Colo.

Andersson, K., Allard, B., Bengtsson, M., Magnusson, B. (1989). *Chemical Composition of Cement Pore Solutions*. Cement and Concrete Research, Vol. 19, No. 3, pp. 327-332. 0008-8846/89.

Andrade, C., Molina, A., Huete, F., Gonzalez, J.A. (1983). *Relation Between the Alkali Content of Cements and the Corrosion Rates of the Galvanized Reinforcements*. In: Crane, A.P. (Editor). Corrosion of Reinforcement in Concrete Construction. London, 13-15 June, 1983. Chichester, UK: Ellis Horwood Limited, 1983, pp. 343-355. ISBN 0-85312-600-3.

Andrade, C., Holst, J.D., Nürnberger U., Whiteley, J.D., Woodman, N. (1992). *Protection Systems for Reinforcement*. Lausanne, Switzerland: CEB, 1992. 82 p. (Bulletin D'Information No 211). ISBN 2- 88394-016-9.

Andrade, C., Holst, J.D., Nürnberger, U., Whiteley, J.D., Woodman, N. (1995). *Coating Protection for Reinforcement*. State of the art report. London, UK: Thomas Telford Publications. 51 p. (CEB Bulletin d'Information 211. 1992) ISBN: 0 7277 2021 X.

Andrade, C., Alonso, C. (2001). *On-Site Measurements of Corrosion Rate of Reinforcements*. Construction and Building Materials, Vol. 15, No. 2-3, pp. 141-145.

Andrade, C., Alonso, C. (2004). *Electrochemical Aspects of Galvanized Reinforcement Corrosion*. In: Yeomans, S.R. (Editor). Galvanized Steel in Reinforced Concrete, Elsevier B.V., Amsterdam, The Netherlands, 2004, 297 p. ISBN 0-08-044511-X.

Arliguie, G. (2001). *Performance of Galvanized Rebar*. COST 521 Workshop, Tampere 17-20 June, 2001. pp. 47-54. Mattila, J. (editor) COST 521. Corrosion of Steel in Reinforced Concrete Structures. Proceedings of the 2001 Workshop, Department of Civil Engineering, Tampere, Finland. 293 p. ISBN 952-15-0634-2.

ASTM A385-03 (2003). *Standard Practice for Providing High Quality Zinc Coatings*. American Society for Testing and Materials, 9 p.

Camitz, G., Pettersson, K. (1989). *Corrosion Protection of Steel in Concrete - Stage 1, Cathodic Corrosion Protection of Steel Reinforcement in Concrete* - The Literature Review. Stockholm, Sweden: Gotab. 70 p. CBI offprint 3:90. Swedish Corrosion Institute, R 63 185: 1989. ISSN 1101-1297 (in Swedish).

Carlos Castillo (2011). *The Electrochemical Behaviour of Zinc.* pp. 1-12

Cast Iron Pipe Research Association (1964). *Soil Corrosion Test Report: Ductile Iron Pipe.*

Corderoy, D.J.H., Herzog, H. (1980). *Passivation of Galvanized Reinforcement by Inhibitor Anions*. In: Tonini, D.E., Gaidis, J.M. (editors). Corrosion of Reinforcing Steel in Concrete. A Symposium on Corrosion of Metals, Bal Harbour, Fla., 4-5 Dec.1978. Philadelphia, Pa, USA: ASTM, American Society for Testing and Materials, pp. 142-159. ASTM stp 713.

DIN 30674-1 (1982-09). *Cement Mortar Coatings For Ductile Iron Pipes - Requirements And Testing.*

Ductile Iron Pipe Research Association (1984). *Handbook of Ductile Iron Pipe*. Birmingham, Ala.

DVGW GW 9:2011 (2011). *Evaluation Of Soils In View Of Their Corrosion Behaviour Towards Buried Pipelines And Vessels Of Non-Alloyed Iron Materials*, pp. 183-194.

El-Mahdy, Gamal Ahmed, Atsushi Nishikata, and Tooru Tsuru (2000). *Electrochemical corrosion monitoring of galvanized steel under cyclic wer-dry conditions*. Corrosion Science.

Esko Sistonen (2009). *Service Life of Hot-dip Galvanised Reinforcement Bars in Carbonated and Chloride-Contaminated Concrete,* pp. 17-33.

Fagerlund, G. (1990), *Durability of Concrete Structures, Summary Review*. 2. Edition. AW Grafiska: Uppsala 1990, 101 p. ISBN 91-87334-00-3 (in Swedish).

Franky Esteban Bedoya Lora (2010). *Corrosion en Suelos*. Colombia

Fuller, A.G. 1981. *Corrosion Resistance of Ductile Iron Pipe*. BCIRA Report 1442. Alvechurch, Birmingham: BCIRA.

Galvanizers' Association of Australia (1999). *After-Fabrication Hot Dip Galvanizing*. A practical Reference for Designers, Specifiers, Engineers, Consultants, Manufacturers and Users – to introduce AS/NZS 4680. Melbourne, Australia, 72 p.

Göran Camitz, Ulf Bergdahl, Tor-Gunnar Vinka (2009). *Stalpalars beständighet mot corrosion i jord. En sammanställning av kunskaper och erfarenheter.* Palkommissionen – Comision on Pile Research.

Gouda, V. K., M. G. A. Khedr, and A. M. Shams El Din. (1967). *Role of anions in the corrosion and corrosion-inhibition of zinc in aqueous solutions*. Corrosion Science. pp. 221-230.

Gustavsberg Rörsystem (2005). *VRS SYSTEM - Ett komplett system rör och rördelar med dragsäkra fogar.*

Ishikawa, Tatsuo, Minori Kumagai, Akemi Yasukawa, Kazuhiko Kanduri, Takenori Nakayama, and Fumio Yuse (2002). *Influence of metal ions on the formation of γ-FeOOH and magnetite rust*. Corrosion Science, pp. 1073-1086.

Ishikawa, Tatsuo, Sho Miyamoto, Kazuhiko Kanduri and Takenori Nakayama (2005). *Influence of anions on the formation of β-FeOOH rust*. Corrosion Science. pp. 2510-2520.

ISO 4179:2005 (2005). *Ductile iron pipes and fittings for pressure and non-pressure pipelines - Cement mortar lining.*

ISO 8179-2. *Ductile iron pipes - External zinc coating - Part 2: Zinc rich paint with finishing layer.*

ISO 8179-1:2004 (2004). *Ductile iron pipes - External zinc-based coating - Part 1: Metallic zinc with finishing layer.*

J. Banach, (1997). *FBE: An End-User's Perspective*, NACE TechEdge Program, Using Fusion Bonded Powder Coating in the Pipeline Industry, Houston, June 1997.

Kehr, A, Dabiri, M, Hislop, R, (2003). *Dual-Layer Fusion-Bonded Epoxy (FBE) Coatings Protect Pipelines*, BHR Group, 15th International Conference on Pipeline Protection, October 29-31, 2003, Aachen, Germany.

Laque, F.R. (1964). *Corrosion Characteristics of Ductile Iron*. Jour. AWWA, 56(11): 1433.

Lichtenstein, Joram (2002). *Coatings for concrete and concrete pipe*. Materials Performance.

Locke, C.E. (1986). *Corrosion of Steel in Portland Cement Concrete: Fundamental Studies.* In: Chaker, V. (editor). Corrosion Effect of Stray Currents and the Techniques for Evaluating Corrosion of Rebars in Concrete, A symposium on Corrosion of Metals, Williamsburg, VA, 28 Nov. 1984. Baltimore, USA: ASTM, pp. 5-14, ASTM stp 906. ISBN 0-8031-0468-5.

Maahn, E., Sorensen, B. (1996). *Influence of Microstructure on the Corrosion Properties of Hot-dip Galvanized Reinforcement in Concrete*. Corrosion (Houston), Vol. 42, No. 4, pp. 187-196. ISSN 0010- 9312.

Marder, A.R. (2000). *The metallurgy of zinc-coated steel*. Progress in Materials Science, Vol. 45, No. 3, pp. 191-271.

Motor Boating & Sailing (1992), *ISSN 0027-1799, 05/1992*, Volume 169, Issue 5.

NACE (1984). *Corrosion Basics: An Introduction*. Houston, Texas: National Association of Corrosion Engineers.

Nürnberger, U. (2000). *Supplementary Corrosion Protection of Reinforcing Steel*. Otto-Graf-Journal, Vol. 11, pp. 77-108.

Peabody, A.W. (1967). *Control of Pipeline Corrosion*. Houston, Texas: National Association of Corrosion Engineers

Porter, F. (1991). *Zinc Handbook, Properties, Processing and Use in Design*. New York, USA: Marcel Dekker, Inc. 629 p. ISBN 0-8247-8340-9.

R. L. Bianchetti, "Economics," A. W. Peabody, R. L. Bianchetti, eds. (2001), *Control of Pipeline Corrosion*, 2nd ed., (Houston, TX: NACE, 2001).

Sears, E.C. (1968). *Comparison of the Soil Corrosion Resistance of Ductile Iron Pipe and Gray Cast Iron Pipe. Materials Protection*, 7(10):33-36.

Sarja, A. et al. (1984). *Zinc-coated Concrete Reinforcement*. Espoo, Finland. VTT, 92 p. Research Reports 306, Technical Research Centre of Finland. ISBN 957-38-2134-X.

SS - EN 545-2006 (2006). *Ductile iron pipes, fittings, accessories and their joints for water pipelines - Requirements and test methods.*

SS - EN 545-2008 (2008). *Ductile iron pipes, fittings, accessories and their joints for water pipelines - Requirements and test methods.*

Vera Cruz, R. P., A. Nishikata, and T.Tsuru (1996). *AC Impedance monitoring of pitting corrosion of stainless steel under wet-dry cyclic condition in chloride-containing environment*. Corrosion Science, pp. 1397-1406.

Vinka, T.-G., Becker, M. (1998). *Corrosion of Galvanised Steel in Concrete*. 1998-08-21. 40 p. Swedish Corrosion Institute, Project Report 63 282:1 (in Swedish).

Yavad, A. P., A. Nishikata, and T. Tsuru (2004). *Electrochemical impedance study on galvanized steel corrosion under cyclic wet-dry conditions – influence of time of wetness.* Corrosion Science, pp. 169-181.

Yeomans, S.R. (1987). *Galvanized Steel Reinforcement in Concrete*. First National Structural Engineering Conference 1987. Melbourne, Australia, 26-28 August 1987. pp. 662-667.

Yeomans, S.R. (1993). *Coated Steel Reinforcement in Concrete*. Part 1. Corrosion Management, Vol. 2, No. 4, pp. 18-29.

Yeomans, S.R. (1994). *A Conceptual Model for the Corrosion of Galvanized Reinforcement in Concrete*. In: Swamy, R.N. (editor). Corrosion and Corrosion Protection of Steel in Concrete. Sheffield, United Kingdom: Sheffield Academic Press Ltd, pp. 1299-1309. ISBN 1-85075-723-2.

Yeomans, S.R. (2004). *Galvanizing of Steel Reinforcement for Use in Building and Construction*. A presentation to a seminar on Galvanized Rebars in Construction and Infrastructure, Mumbai, India, 27 October, 2004.

Yeomans, S.R. (2004). *Galvanized Steel in Reinforced Concrete*. Elsevier B.V., Amsterdam, The Netherlands, 297 p. ISBN 0-08-044511-X.

8 LIST OF TABLES

9 LIST OF FIGURES